Volume 3
Number 13
7 July 2021
Pages 3653–3968

Nanoscale Advances

rsc.li/nanoscale-advances

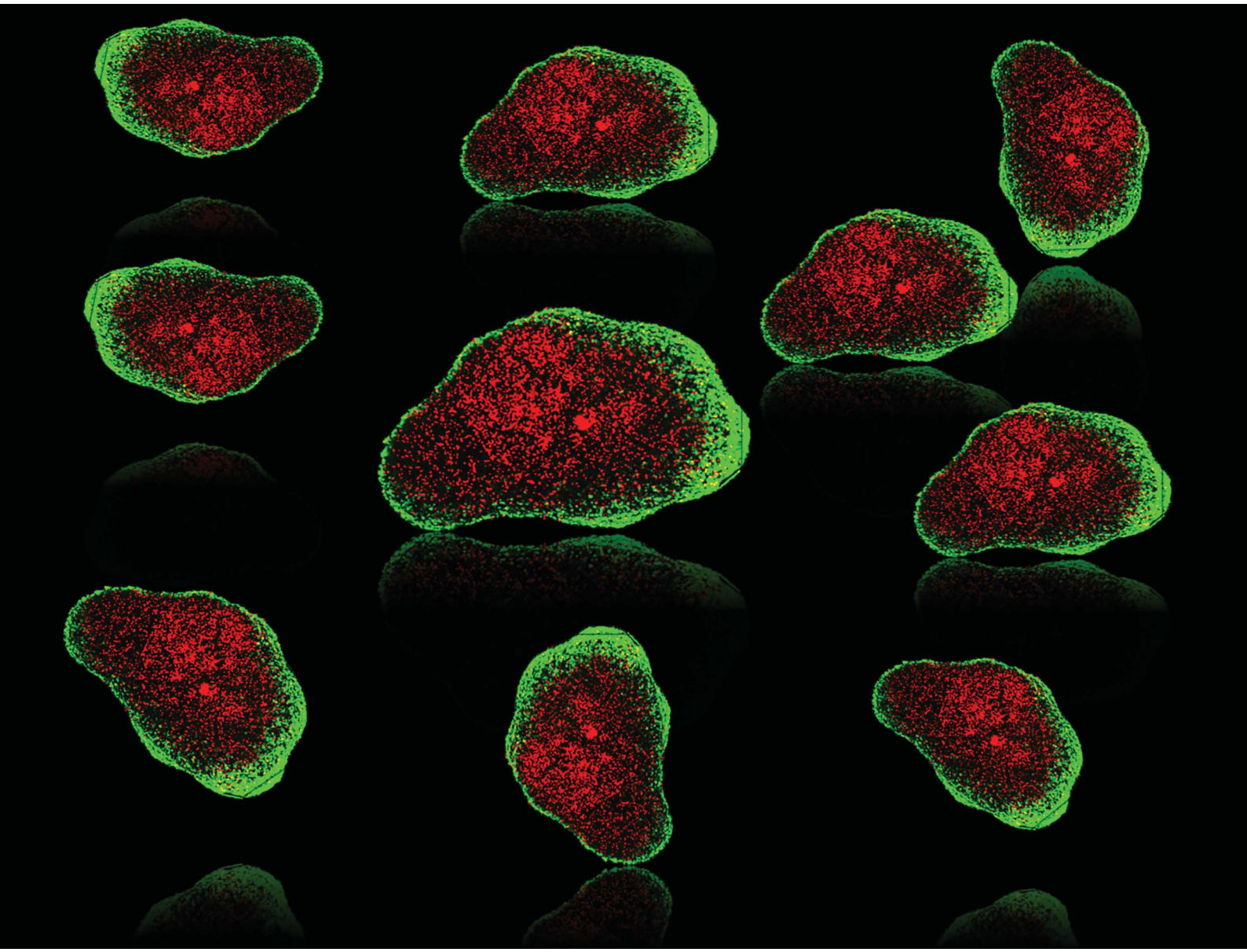

ISSN 2516-0230

ROYAL SOCIETY OF CHEMISTRY

REVIEW ARTICLE
Ruby Gupta and Deepika Sharma
Therapeutic response differences between 2D and 3D tumor models of magnetic hyperthermia

NCNST

Nanoscale Advances

REVIEW

View Article Online
View Journal | View Issue

Cite this: *Nanoscale Adv.*, 2021, **3**, 3663

Therapeutic response differences between 2D and 3D tumor models of magnetic hyperthermia

Ruby Gupta and Deepika Sharma *

Received 24th March 2021
Accepted 5th May 2021

DOI: 10.1039/d1na00224d

rsc.li/nanoscale-advances

Magnetic hyperthermia-based cancer therapy (MHCT) has surfaced as one of the promising techniques for inaccessible solid tumors. It involves generation of localized heat in the tumor tissues on application of an alternating magnetic field in the presence of magnetic nanoparticles (MNPs). Unfortunately, lack of precise temperature and adequate MNP distribution at the tumor site under *in vivo* conditions has limited its application in the biomedical field. Evaluation of *in vitro* tumor models is an alternative for *in vivo* models. However, generally used *in vitro* two-dimensional (2D) models cannot mimic all the characteristics of a patient's tumor and hence, fail to establish or address the experimental variables and concerns. Considering that three-dimensional (3D) models have emerged as the best possible state to

Institute of Nano Science and Technology, Knowledge City, Sector 81, Mohali, Punjab-140306, India. E-mail: deepika@inst.ac.in

Ruby Gupta received her Masters of Research degree in Cancer Biology from University of Dundee, United Kingdom in 2013. Following a Senior Research Fellowship in Department of Haematology from Post Graduate Institute of Medical Education & Research, Chandigarh, India from 2013 to 2015, she joined the Institute of Nano Science and Technology (INST) as a Doctorate student in 2016. She is currently a part of the Chemical Biology group at INST. Her main research interests include synthesis and application of magnetic nano-heaters for theranostic therapy of solid tumors.

Dr Deepika Sharma has more than eight years of post-PhD research experience and is working in the area of Cancer Nanotechnology in a Scientist 'C' position at the Institute of Nano Science and Technology (INST). She has established her laboratory that is largely supported by her ECR project funded by DST-SERB. She has established both in vitro and in vivo hyperthermia facilities at INST to carry out magnetic hyperthermia based cancer therapy work till pre-clinical levels. Dr Sharma is working on the study of cancer therapy through the development of a broad range of impactful nanosystems that can be used to detect, monitor, or enhance cancer treatment, particularly focusing on hyperthermia and its contribution towards cancer prevention. This is an emerging field and not many people in India are working on these aspects, especially worth mentioning that she has started this activity in INST Mohali. She is also involved in understanding the biological phenomena that include the synthesis of nano-transducers movement through biological barriers to fight against inoperable tumours. She has published more than 20 papers and 1 book chapter with more than 800 citations in highly reputed international and national journals, such as Trends in Biotechnology, Biotechnology Advances, International Journal of Hyperthermia, ACS Applied Nanomaterials, Food Chemistry, Dalton Transactions, Journal of Radiation and Cancer Research, etc.

replicate the *in vivo* conditions successfully in the laboratory for most cell types, it is possible to conduct MHCT studies with higher clinical relevance for the analysis of the selection of magnetic parameters, MNP distribution, heat dissipation, action and acquired thermotolerance in cancer cells. In this review, various forms of 3D cultures have been considered and the successful implication of MHCT on them has been summarized, which includes tumor spheroids, and cultures grown in scaffolds, cell culture inserts and microfluidic devices. This review aims to summarize the contrast between 2D and 3D *in vitro* tumor models for pre-clinical MHCT studies. Furthermore, we have collated and discussed the usefulness, suitability, pros and cons of these tumor models. Even though numerous cell culture models have been established, further investigations on the new pre-clinical models and selection of best fit model for successful MHCT applications are still necessary to confer a better understanding for researchers.

1. Magnetic hyperthermia and the role of the tumor microenvironment

Magnetic hyperthermia is a promising technique for cancer treatment wherein the tumor cells are exposed to an externally applied alternating magnetic field (AMF) in the presence of magnetic nanoparticles (MNPs). The AMF application induces localized heat in the tumor tissues, raising the temperature to 42–45 °C, at which cancer cells are killed specifically, while healthy cells remain unaffected.[1,2] Besides this magneto-selectivity, the capability to penetrate deep inside the tumor mass forms another major advantage of the MHCT modality as compared to the other treatment regimens including chemotherapy, radiotherapy and surgery.[3] Magnetic hyperthermia-mediated cancer therapy (MHCT) was first performed by Gilchrist *et al.*, in 1957 (ref. 4) by heating maghemite nanoparticles (20–100 nm sized) at 43–46 °C using 1.2 MHz AMF to tackle metastasis in lymphatic nodes. Since then, MHCT has been explored for treatment of various malignancies with MHCT-based clinical trials being underway for prostate, brain, head and neck and esophagus cancers.[5]

Although MHCT is being exploited in clinical trials, further in-depth understanding and research are required to fully realize the therapeutic potential of the nano-theranostic technique. The proper functionality of MNPs for MHCT depends on their intrinsic magnetic properties (saturation magnetization and Curie temperature) as well as biophysical properties (biocompatibility, colloidal stability, and heat generating capabilities). The magnetic heat dissipations achieved from MNPs are also dependent on the geometrical features of the MNPs such as the particle size, composition, shape and surface chemistry along with AMF parameters, such as frequency, field strength and duration of AMF exposure.[1–3] Thus, with an aim to

Table 1 Comprehensive summary of the advancement in MNP design for the MHCT study

Nanosystem	Size (nm)	Coating	M_s (emu g^{-1})	AMF		SAR (W g^{-1})	Cell line targeted	Ref.
				f (kHz)	H (Oe)			
$La_{0.7}Sr_{0.3}MnO_3$	45	Tetraethyl orthosilicate	42	350	176	255	Lung (A549)	6
$Ho_xFe_{3-x}O_4$	10–15	Citric acid	—	488	300	337.3	—	7
$Mn_{0.6}Ga_{0.4}Fe_2O_4$		Pluronic F127	30.2	354	128	160.9	—	8
Fe_3O_4	21	Cetyltrimethylammonium bromide and polycaprolactone	64	312–326	198–790	255.12	Liver (HepG2)	9
Fe_3O_4	100	Aminosilane	—	557	300	320	Glioblastoma (C6)	10
Fe_3O_4	21	Dextran	43	150	150	52.3	Breast (MC4-L2)	11
Fe_3O_4–γFe_2O_3	10–14	Polyphenol	70.84	570	300	—	Microglial (BV2)	12
Fe_3O_4	27	—	37.5	13 560	—	725	Glioblastoma (C6)	13
$Mn_xFe_{3-x}O_4$	34	Citric acid	—	405	168	—	Glioblastoma (C6)	14
Fe_3O_4	3	Stevioside	—	405	168	80	Glioblastoma (C6)	15
Fe_3O_4	45	Oleic acid	—	265	335.2	80	Breast (MCF7)	16
$MnFe_2O_4$	18	Chitosan	58.34	307	754	270	Breast (MDA-MB-231)	17
$NiFe_2O_4$	16	Polyethylene glycol	15	260	49–69.11	17–22	—	18
Fe_3O_4	14	Phosphate	63.6	126	10.3	11.1	—	19
$MnFe_2O_4$	14	Tetraethyl orthosilicate	40	260	69.11	47.84–84.65	—	20
$Zn_{0.9}Fe_{0.1}Fe_2O_4$	11	—	12	700	34.4	36	Glioblastoma (U87-MG)	21
$Fe_{68.2}Cr_{11.5}Nb_{0.3}B_{20}$	20–40	Chitosan	42	153	3500	215	Osteosarcoma	22
$Co_xFe_{3-x}O_4$, $0 < x < 1$	8	—	72	183	151	6.5–40.4	—	23
γ-Fe_2O_3	32	—	55	394	301.5	193	—	24
Fe_3O_4	15	Chitosan	49.9	265	335.2	118.85	Fibroblasts (L929)	25
$MgFe_2O_4$	12	Dextran	33.83	256	335.2	85.57	Fibroblasts (L929)	26
$La_{0.7}Sr_{0.3}MnO_3$	25	Oleic acid	35	265	335.2	46	Human negroid cervix epitheloid carcinoma (HeLa)	27

maximize the specific absorption rate (SAR) *i.e.* the measure of heat dissipated per unit mass of the nanoparticle, various properties of MNPs have been investigated which include their route of synthesis, particle–particle interactions, and size and morphology of nanomaterials. Many synthesized MNPs with varied characteristics and magnetizations for pre-clinical MHCT applications have been studied. Table 1 shows a comprehensive classification of different types of MNPs designed for MHCT study against various cancers. However, the understanding of biological effects of the localized heat generated at tumor tissues in a cellular environment still requires a significant amount of research work. Fig. 1 shows the schematic layout of limited understanding of how magnetic hyperthermia affects tumor progression at the sub-cellular level.

Despite these advancements, various drawbacks of MHCT still limits its unparalleled application in biomedical field. Some of these limitations include requirement of optimization of the magnetic field parameters, amount of MNPs administered, delivering an effective dosage of MNPs at the tumor site and precise measurement of temperature at the localized tumor tissues.[1,28] Hence, a major concern for clinical translation of such nanotechnology-based therapies involve attaining the desired therapeutic hyperthermia window with the lowest amount of MNPs at lower frequency and field strength.

One of the major challenges limiting the use of MHCT is the underestimation of the role of the tumor microenvironment (TME) in developing thermotolerance in cells. The TME comprises the various infiltrating host cells, extracellular matrix (ECM) components and secreted factors like growth factors, cytokines, interleukins and chemokines (*e.g.* VEGF, IL-8 and tumor necrosis factor) besides the heterogeneous cancer cell population residing in the tumor mass.[29,30] The crosstalk between the TME and tumor cells is known to profoundly influence the rate of tumor progression. It can also define therapeutic responses and resistance, thus justifying the recent thrust to target the TME components.[31,32] Most of the published data regarding MHCT is based on experiments performed in two-dimensional (2D) conditions where cells are grown on rigid and flat surfaces, typically made of glass and polystyrene. These traditional cell monolayer cultures, maintained under simplified and laboratory conditions, fail to fully reflect the essential physiology of tissues. Upon 2D culturing, the tissue-specific architecture and functions are modified in terms of altered cell shape, forced polarity, biochemical signaling and the subsequent cell–cell and cell–microenvironment communication.[33,34] Despite these drawbacks, laboratory based *in vitro* 2D experiments are used to evaluate the cellular processes owing to their ease of simplicity and application, reasonable cost and precise control over the microenvironmental factors.[35] For a further in-depth confirmation of a physiological process or a mechanism observed *in vitro*, the conventional approach is to test the system in standard animal models, referred to as *in vivo* tumor models. However, there may be substantial inconsistencies in the results obtained when the *in vitro* experimental parameters decided in 2D cultures are employed for *in vivo* models. Moreover, various concerns regarding the distress or the pain of animals under certain experimental procedures exist. Many experimental animals are immunosuppressed and do not exhibit the same interactions between tumor and stromal cells as those observed in humans, which hinders the translation of laboratory research to clinical applications.[36] Hence, obtaining concordance between *in vivo* experiments and clinical trials still remains a challenge.[37,38] One possible way of bridging this gap is to use three-dimensional (3D) *in vitro* tumor models to better mimic the complexity of tumor biology.[39] In 3D *in vitro* models, the cells are grown as aggregates of either single or multiple cell types which promotes cellular proliferation in a geometrical fashion, stimulating production of ECM and thus, enhancing the cell–cell contact and communication.[40–42] Fig. 2 represents the morphological differences observed for rat glioma C6 cells under different cultural conditions in our lab using scanning electron microscopy (JSM-IT300, Jeol Ltd, Japan). As depicted in the figure, cells display flat morphology with attachment to the surface (glass cover slip in this case) when grown in 2D cultures and as aggregates of single cells forming spheroids (magnified view shown) when grown as 3D cultures on agarose gels. The morphological depiction of cells observed in 3D closely mimics the clustered tumor mass found under *in vivo* conditions (Fig. 3). 3D cultures can thus mimic both the physiological geometry of the malignant tissue and also its interaction with the tumor microenvironment to which the cancer cells are exposed that ultimately decides the fate of tumors when subjected to AMF (*e.g.*, survival, progression, heterogeneity in gene expression and drug resistance).[43–45] The ideal *in vitro* 3D tumor model could thus closely resemble the patient's tumors

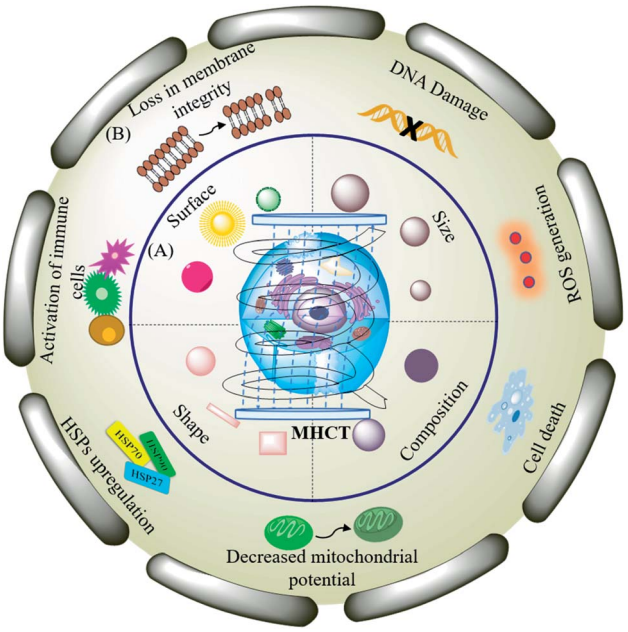

Fig. 1 Schematic representation of the mechanism of magnetic hyperthermia at the sub-cellular level (A) using optimized nanosystems by altering their size, composition, shape and surface chemistry; (B) understanding the effect of loacalized heat at the sub-cellular level by disrupting the membrane integrity/structure, induction of DNA damage and apoptotic cell death, ROS generation, decreased mitochondrial membrane potential, upregulation of heat shock proteins (HSPs) and activation of immune cells in the tumor microenvironment.

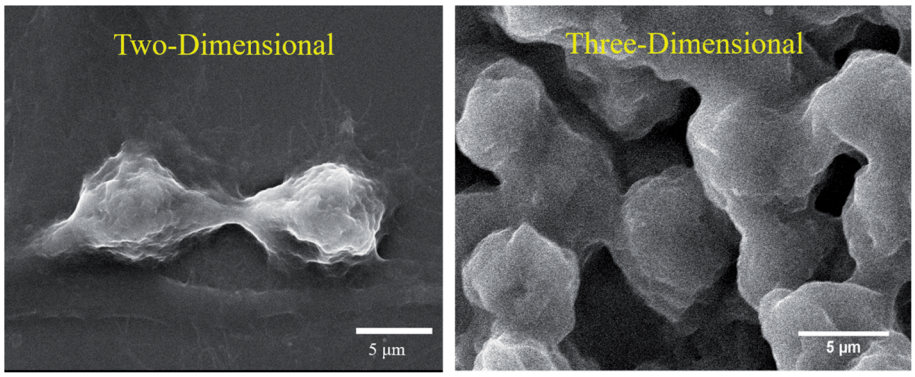

Fig. 2 Representation of cellular morphology of rat glioma C6 cells under 2D and 3D cultural conditions as observed by scanning electron microscopy in our lab. Cells were cultured on a glass coverslip in case of 2D (left panel) or on agarose gel to form 3D spheroid cultures (right panel). Scale bar = 5 μm.

eliminating the therapeutic differences observed as we move from *in vitro* testing to clinical applications of MHCT. 3D culturing would further allow simultaneous testing of numerous variables for an optimized hyperthermia treatment to be applied directly to human samples, thus establishing MHCT as the sole therapy regime for malignancies across the scientific community.[35]

To promote the research for an efficient MHCT approach at the pre-clinical level, the establishment of a reliable and validated 3D tumor model would be of keen interest. So, this article is focused on the caveats and suitability of using 3D over 2D *in vitro* models, specifically in MHCT applications.

2. Differences in therapeutic responses between 2D and 3D culturing

2.1 Differences in the tumor microenvironment (TME)

The exchange between the tumor microenvironment (TME) and the tumor cells has evolved as a foremost challenge for predicting outcomes of cancer therapies owing to the complexity and heterogeneity of various tumors.[46,47] The TME is comprised of various non-malignant cell types and their stroma, such as fibroblasts, cells of the immune system (T-cells, B-cells, NK-cells and macrophages), mesenchymal cells, and endothelial cells, which all have a specific role in the progression or regression of the tumor.[48] Probing interactions between tumor cells and cellular components of the TME forms a platform where the complex features of tumors, such as proliferation, metastasis and chemoresistance can be inspected.[35]

However, the TME may vary under different culture conditions (Fig. 3). Under 2D culture conditions, cells grow as monolayers with forced polarized cell adhesion and limited contact with adjoining cells. This growth pattern allows them to get a homogeneous supply of oxygen, nutrients and growth factors present in the media, which results in abnormal cell growth and distribution of cell surface receptors in an unrealistic manner, which is consequential for them to fail to mimic the natural *in vivo* conditions (Fig. 3(A)). These limitations have encouraged the development of many 3D *in vitro* models to

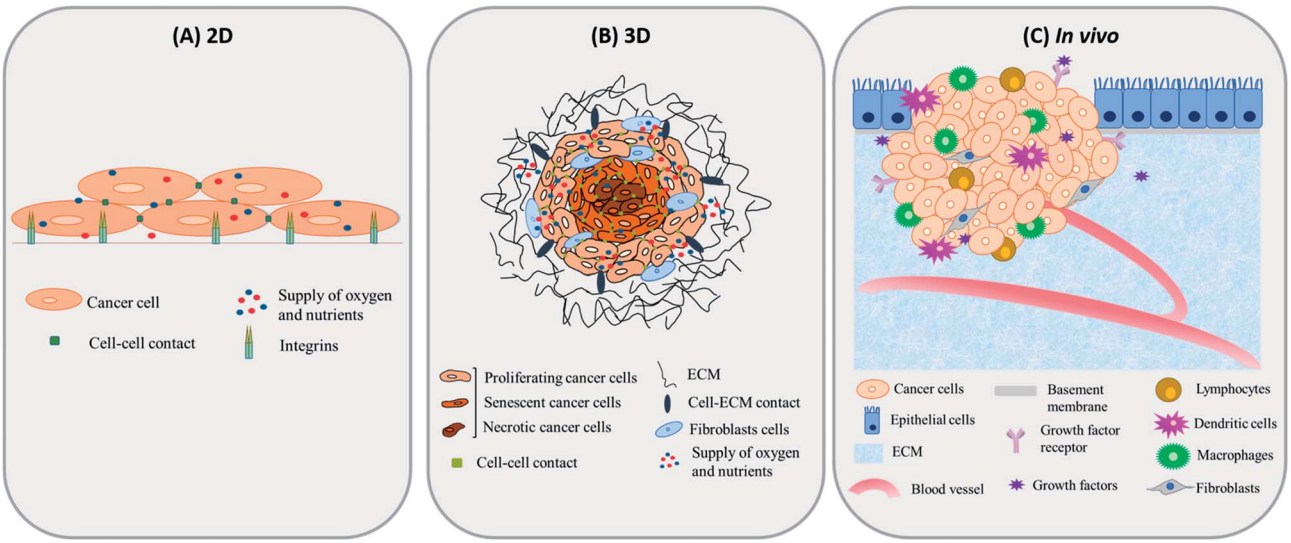

Fig. 3 Tumor microenvironment under different culture conditions *i.e.* (A) 2D, (B) 3D and (C) *in vivo* conditions.

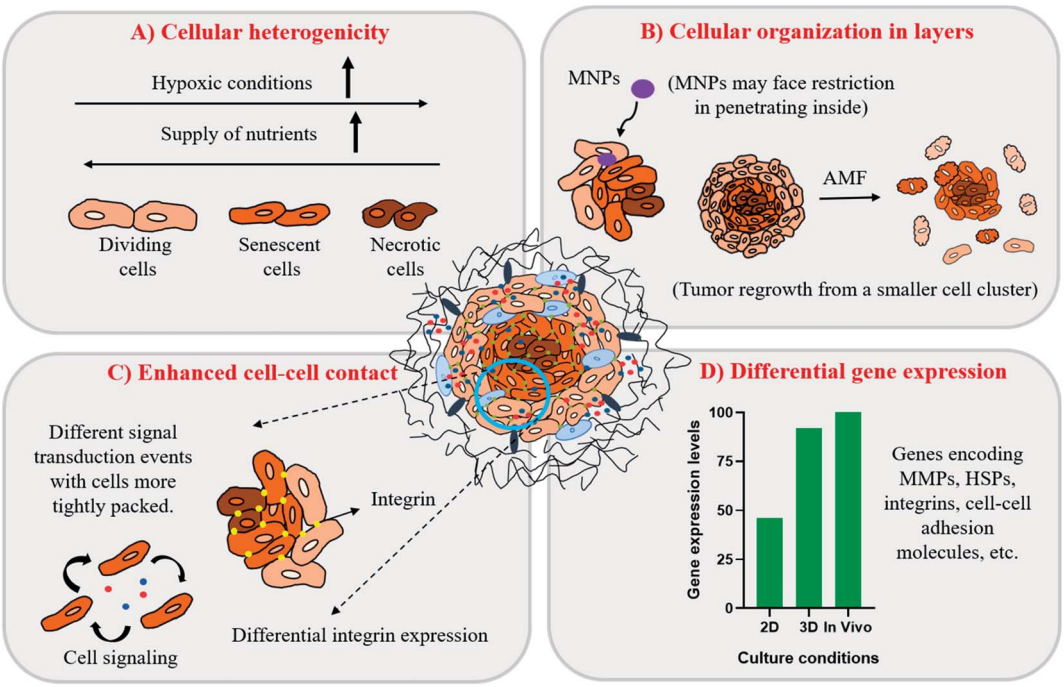

Fig. 4 Characteristics of 3D cultures as represented by tumor spheroids. (A) Cells are organized in a heterogenous arrangement, mainly in three layers (dividing, senescent and necrotic cells) owing to differential supply of nutrients and oxygen within the cells packed in the inner core which resembles that observed in patient tumors. (B) Tightly packed cellular organization in spheroids hinders penetration capability of drugs or nanoparticles leading to non-uniform distribution in tumors. Cellular organisation also favors tumor re-growth from a small cellular cluster resulting from lesser damage to cells on AMF application. (C) Enhanced contact between various cells (cancer–cancer and cancer–stromal cells interaction) reproduces the integrin distribution and signal transduction pathways found under *in vivo* conditions. (D) Representation of differential gene expression levels obtained from cultures grown in 2D, 3D and *in vivo* conditions.

better mimic the complex pathophysiological characteristics of the TME *in vitro* (Fig. 3(B and C)).

In 3D *in vitro* tumor models, as represented here by a spheroid (Fig. 4, key figure), many studies have shown that such tumor spheroids display complex architecture with heterogeneous cell morphologies *i.e.* the cellular organization of spheroids commonly is in 3 layers (Fig. 4(A)):[49,50]

(i) An innermost hypoxic core with mainly necrotic cells.

(ii) A middle layer comprising of senescent cells and.

(iii) An outer layer of proliferating cells.

Hence, with this proliferation gradient, the 3D cultures represent better approximation of tumor heterogenicity as observed under *in vivo* conditions. The level of oxygen and nutrients is lower in the inner core due to highly compact cell density and increased ECM secretion, which successfully translates the *in vivo* tumor conditions.[35] The hypoxic environment in the core leads to an increased amount of glycolysis producing lactate to obtain energy by a process called the Warburg effect.[51] The accumulation of lactate in spheroids further results in acidification of its interior (pH of 6.5–7.2), a phenomenon that also occurs within the *in vivo* tumor microenvironment.[52,53] The arrangement of cells in three different zones also leads to variable heat sensitivity among the layers, as demonstrated by increased thermo-sensitivity in the nutrient-depleted monolayer cultures which closely resemble the cells present in the innermost nutrient-depleted necrotic zone of the spheroids with higher thermo-sensitivity.[54] This is further supported by the independent observation of enhanced central necrotic zone diameter after hyperthermia treatment by Sutherland and group.[55] In accordance with this, we have also observed an increase in central necrotic zone of rat glioma C6 spheroids on the application of AMF of strength 168 G and frequency of 405 kHz for 20 min using a DM2 equipped-DM100 heating system (nB nanoscale Biomagnetics Spain). The results were visualized by the live/dead assay using a Zeiss LSM880 confocal microscope (Carl Zeiss, Thornwood, New York) (Chart 1).

In addition to the proliferation gradient, the drug concentration gradient also exists in 3D cultures owing to the tight compact packing of cells in the spheroids.[35] Such drug heterogenicity in 3D models is conducive to variations in therapeutic responses to MHCT achieved as compared to responses in 2D cultures. As depicted in Fig. 3(B), the barrier formed by the cancer-associated fibroblasts cells, mainly the ECM–cell barrier (α5- and β1-integrin) and cell–cell contact (E-cadherins) can limit the amount of drugs or nanoparticles penetrating inside the spheroids.[56,57] One study investigated the combinatorial effect of a melanogenesis-targeting drug, *N*-propionyl-4-cysteaminylphenol (NPrCAP), and exogenous heat therapy (42 °C for 60 min) on 3D culture of melanoma (B16F1) cell spheroids formed in collagen gel.[58] The melanogenesis of B16F1 cells was found to be 29-fold higher in the 3D cultures than that

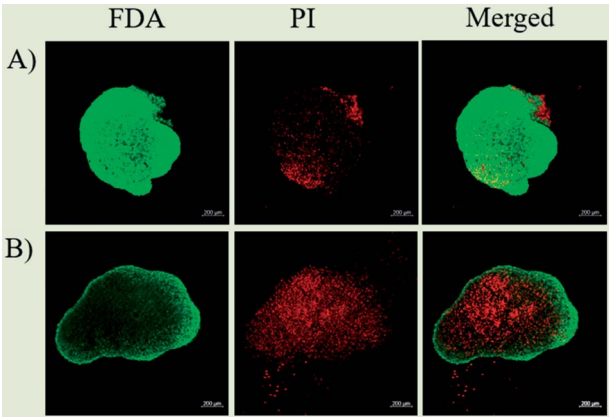

Chart 1 Live/dead assay to study the effect of MHCT on C6 spheroids. Live/dead assay on C6 tumor 3D cultures representing (A) untreated cells and (B) cells exposed to AMF (405 kHz and 168 G) for 20 min. The AMF exposure resulted in enhancement of central necrotic zone area in the spheroids as seen by increased uptake of propidium iodide (PI) dye. Live cells were stained green using Fluorescein diacetate (FDA; Invitrogen) and dead/necrotic cells were stained red using propidium iodide (PI; Invitrogen) Scale bar = 200 μm.

observed in the 2D environment. Also, the IC_{50} value of NPrCAP coupled with heat treatment was observed to be 2-fold higher in the 3D cultures (0.30 mM) than in 2D monolayer cultures (0.15 mM). The results achieved indicate that spheroid formation reduces the chemosensitivity of cancer cells as promoted by cancer–stromal cell signaling, thus presenting as a better screening platform for the *in vitro* studies.[47,59] Another study by Brüningk and group, reported tumor re-growth of two different cancer cell lines, namely colorectal (HCT116) and squamous cell carcinoma (CAL27) cultured as spheroids, while the monolayers of both the cell lines exhibited no such tumor re-growth after heat exposure.[42] Thus, indicating that the heat response is governed by factors specific to the culture conditions, such as the cellular environment or enhanced contact between cells in 3D cultures (Fig. 4(C)).

ECM-related signaling pathways, particularly, ECM–cell exchanges can influence tumor progression by altering the expression of proteinases (*e.g.*, metalloproteinases (MMPs)) that can modify the ECM structure and thus promote cancer cell migration and invasion to other tissues.[60,61] Other cell targets include cell surface molecules like integrins which form the main cell adhesion receptors that play a vital role in cell signaling, cell migration and are thus associated with primary benign tumors translation to malignant tumor mass.[62,63] However, the expression of such a crucial tumor fate deciding factor is known to vary under different cultural conditions. Cells grown in monolayers exhibit fewer cell–cell contacts with integrin clustering while, growth in 3D promotes clustered cell growth with enhanced cell–cell contact points, and homogenous distribution of integrins across the cell membrane in association with ECM proteins.[64] This lack of integrin clustering likely leads to different signal transduction events in 3D cultures as compared with those grown in 2D (Fig. 4(C)). For example, studies have reported ECM-β1 integrin interaction to play a vital role in regulating growth and progression of PC3 prostate carcinoma cell line in 3D cultures, while depletion of β1 integrin had no such effect on the growth of PC3 cells in 2D.[65] Such differential signal transduction events depending upon the culture conditions can result in false prediction of the therapeutic outcome in 2D cultures. Thus, hindering the understanding of the true molecular pathogenic pathways involved in cancer cells treated with heat or other adjuvant therapies.

Besides the expression of cell surface molecules and variable cell signaling pathways, gene expression profiles of various proteins are also strongly affected by the 3D cellular organization characteristic of cancer cells.[41] Unlike the expression in 2D cultures, the gene expression pattern observed in spheroids has been found comparable to those achieved in solid tumors *in vivo* (Fig. 4(D)).[66–69] To validate this, Ghosh and co-workers have reported over-expression of genes responsible for skin cancer progression and metastasis in 3D cultures as compared to the conventional 2D cultures of melanoma cells.[66] Kumar *et al.* have also reported expression of several proteins involved in metabolic activity, signal transduction, cytoskeletal components, transport polypeptides and heat stress to be upregulated in spheroids as compared to in monolayer cultures of neuroblastoma solid tumor cells by two-dimensional polyacrylamide gel electrophoresis.[67] In addition, similar results have also been

Table 2 Comparison of 2D and 3D *in vitro* tumor models

Properties	2D	3D
Morphology	Forced polarization, leading to shape change	Conserved polarization with true shape intact
Tumor heterogenicity	Uniform	Existence of cell proliferation and drug gradients
Gene expression	Altered expression of genes observed	Better representation of proliferation, cell signaling proteins and other growth factors expression levels
Differentiation of cells	Non-spontaneous	Could be spontaneous due to increased cell–cell and/or cell–ECM interactions
Angiogenesis	Non-functional (observational only)	Could be functional
Cost	Cheap	Increases as more components are added
Reproducibility	Consistent with slight variation	Difficult
Resemblance to *in vivo* tumor models	Negligible	Comparatively higher

reported for 3D tumor spheroids mimicking liver hepatocellular carcinoma;[68] mesothelioma[69] and colorectal cancer.[70] Table 2 presents a comparison of the properties of cells grown under 2D and 3D conditions.

Overall, all the above mentioned *in vitro* 3D tumor characteristics (Fig. 4) present an important link for successful translation of *in vitro* cultures to ideally mimic the precise 3D microenvironment of *in vivo* tumors.

2.2 Differences in the heat stress response between 2D and 3D cultures

The heat stress response to MHCT by practically all cells and tissues is exhibited by the heat shock proteins (HSPs) expression in a devised way to rescue the denatured proteins and promote cell survival.[71] Most of the HSPs behave as molecular chaperones to repair the consequences of heat stress to other cellular proteins namely protein aggregation, misfolding or disruption of regulatory complexes. The mammalian family of HSPs can be broadly classified into five categories corresponding to their molecular size: HSP100, HSP90, HSP70, HSP60, and other small HSPs (15–30 kDa). The expression of these HSPs is upregulated in response to sublethal stressful stimuli like osmotic stress,[72] hypoxia,[73] heat stress,[74] ionizing radiation[75] and mechanical stress[76] (Fig. 5(A)). The characteristic preferential up-regulation of HSPs is part of a greater stress recovery process that activates the cellular mechanisms to promote survival after an initial insult.[74,77] The heat shock response is mainly regulated by a family of transcription factors among which the heat shock factor 1 (HSF1) comprises the main regulator of HSP expression. Upon activation by stress stimuli, HSF1 is translocated from the inactive monomeric state in the cytoplasm to the homo-trimerized state in the nucleus, where it binds to the heat shock elements (HSEs) located upstream of the HSP gene promotor to induce the HSPs gene transcription (Fig. 5(B)).

However, the heat stress response may vary for cultures grown under different conditions. The cells grown in the 2D environment are subjected to nearly uniform distribution of MNPs throughout the surface of the tissue culture dish. However, in the 3D microenvironment, the cellular distribution of MNPs is far from uniform owing to the organizational behavior of tumor cells which is conducive to hypoxic conditions with poor vascularization within the necrotic cores[78] (Fig. 4). On heat stress (by AMF application or by other means), cells cultured in 2D generally face more mechanical damage with significant cell death[14,15] while the tumor spheroids generated in 3D form distorted structures with enhanced central necrotic zone and lower decrease in cell viability (Fig. 5(C)).[35] In support of this, Durand (1978) has reported acquired thermotolerance in Chinese hamster V79 cells as spheroids relative to those heated in monolayer cultures at temperatures >43 °C using an exogenous water bath.[79] The different levels of HSP expression, as discussed in Section 2.1 (Fig. 4(D)) could be a plausible reason for such observed therapeutic differences between 2D and 3D cultures. In accordance with this observed effect, a study reports the expression of HSP27 to be dependent upon the culture conditions of the cells with higher expression in cells grown in the 3D environment.[80]

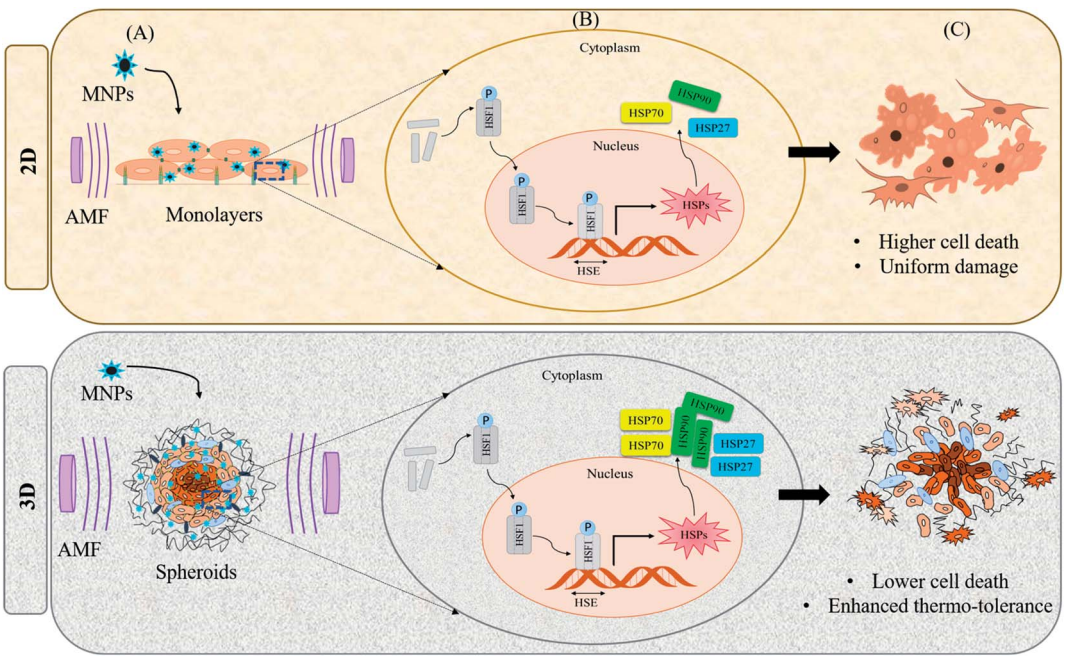

Fig. 5 Differential heat shock response under 2D and 3D culture conditions. (A) On application of AMF to cells cultured under 2D or 3D conditions, heat stress response is activated which induces differential expression of HSPs depending upon the culture conditions; (B) HSF1 denotes transcription factor for HSPs (heat shock factor 1); HSE denotes heat shock elements (DNA binding domain for HSF1); (C) heat stress under 2D conditions causes higher cell death as cells are exposed to AMF uniformly while under 3D conditions, cells acquire higher thermotolerance owing to enhanced expression of HSPs.

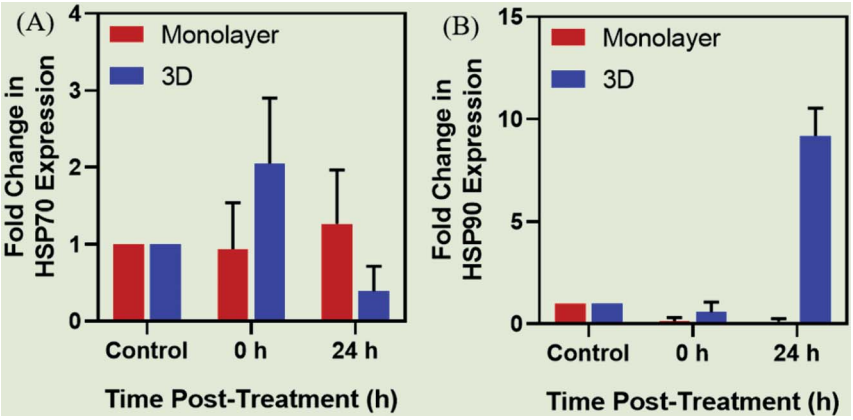

Chart 2 Expression analysis of HSPs under different culture conditions. Time-dependent comparative gene expression analysis of (A) HSP70 and (B) HSP90 as expressed in monolayers and 3D tumor spheroids of C6 glioma cells after exposure to AMF of strength 168 G and 405 kHz for 20 min.

Similarly, another study reported comparative expression analysis of expression levels of HSP70 in prostate cancer cells (PC3) grown in 2D and 3D culture environments.[74] They also evaluated the incidence of cell death mechanisms *i.e.* apoptosis and necrosis of PC3 in response to hyperthermia. To induce controlled hyperthermia, the cells were exposed to an exogenous heat source – water bath maintained in the temperature range of 37–57 °C for a period up to 2 h. The results indicated reduced cell death incidence in cells grown in 3D cultures than those grown as monolayers with higher expression levels of HSP70 in response to heat stress. We have also observed such differential expression of HSPs, namely HSP70 and 90, after AMF application (168 G and 405 kHz) for 20 min using a DM100 nano-magnetic heating system (nB nanoscale Biomagnetics, Spain) under different culture conditions *i.e.* monolayer and 3D cultures of rat glioma C6 cells (Chart 2). The expression analysis was done immediately after AMF exposure as well as after 24 h of re-culturing cells post-heat stress to analyze the long term effects of the therapy. As represented in the figure, the expression level of both HSPs was observed to be time-dependent with higher thermo-tolerance attributed in 3D cultures with higher expression of HSPs.

Various studies have indicated the increased expression of HSPs to be involved in the establishment of the malignant phenotype, including programmed cell death inhibition, sustaining angiogenesis, and reducing chemosensitivity.[1,81–84] HSPs are essential for the survival and progression of neoplastic cells and thus, represent potential targets for anti-cancer therapy. Understanding the mechanisms and the cellular signaling machinery involved to inhibit up-regulation of these self-defensive HSPs gene expression by cancer cells can widely enhance the long term efficacy of MHCT. In this regard, various studies have reported use of small molecule drug inhibitors of HSPs like Pifithrin-mu and Quercetin against HSP70,[85,86] Geldamycin or its less toxic derivatives like 17-AAG against HSP90;[87–89] anti-HSPs targeted antibodies against extracellular or membrane-bound HSPs.[90,91] Machida *et al.* investigated and compared radiosensitization of human squamous cell carcinoma cell lines grown both as monolayers and as multicellular spheroids on inhibition of HSP90 by 17-AAG after X-ray irradiation (6 Gy) using a linear accelerator (Mitsubishi Medical Linac, Mitsubishi Electric, Japan).[87] 17-AAG enhanced the radiosensitization of the cancer cells both in monolayers and spheroids however, a higher concentration of 17-AAG was required for spheroids (1 μM) as compared to that for monolayers (0.2 μM) to achieve similar cancer cell death. Similarly, Matokanovic and group reported simultaneous inhibition of HSP70 and 90 to enhance the glioma cell death using Hsp70 siRNA and celastrol as the HSP90 inhibitor.[92] The results indicated that higher concentrations of both celastrol and Hsp70 siRNA were necessary to induce comparable cell death as that observed in monolayer cultures. The need for higher dose of HSP inhibitors in 3D cultures to achieve comparable therapeutic outcomes with that in 2D could be attributed either to higher expression levels of HSPs and/or to the inefficient distribution of the drugs into the tumor cluster in the former case.

Hence, with HSPs being held conducive for the acquired thermo-tolerance in cancer cells on heat stress, their overexpression in spheroids facilitates the notion that the *in vivo* tumor microenvironment is better accounted for in *in vitro* 3D models. These differences thus highlight the importance of selecting physiologically relevant 3D *in vitro* tumor models in assessing true therapeutic responses of MHCT in experimental settings to effectively evaluate and optimize the potential of the therapy regime.

3. Successful 3D *in vitro* tumor models for MHCT

Various groups have reported therapeutic response of MHCT in 3D *in vitro* tumor models. 3D culturing has been performed for multiple applications including generation of tumor spheroids, culture growth in microfluidic devices to generate organs-on-a-chip, culturing tumor cells on cell culture inserts and embedding cells in 3D tissue scaffolds. The detailed 3D *in vitro* tumor models with their successful implications for MHCT are discussed below.

3.1 Tumor spheroids

Despite the advantages of 3D culturing over 2D cultures, the number of studies using 3D cell culture models to investigate the therapeutic effect of MHCT is still scarce as of now.[93] Most of these limited studies have mainly investigated tumor spheroids as 3D cell cultures.

A magneto-responsive energy/drug carrier system that promotes deep tumor penetration using lactoferrin-capped mesoporous MNPs for therapy of a 3D brain cancer model (RG2 cells) was generated by Su *et al.* (2015).[57] For the chemo-magneto combinatorial therapy, both perfluorohexane (PFH) and Paclitaxel (PTX) drugs were loaded into porous structures of NPs. The cytotoxic effect of both short and longer duration of magnetic field of strength 50 Oe and 50 kHz was evaluated. Short-duration (1 min) magneto-triggered PFH release was able to cause destruction of tumor spheroids, enhancing the drug penetration depth and concentration accumulated in deep tumors. Whereas, long-duration MF treatment (5 min) further led to generation of intense heat with a burst-like drug release in tumor spheroids, causing reduction of cell viability to just 4% as a result of the thermo-chemo-therapy.

Stocke *et al.* (2017) reported evaluation of the *in vitro* theranostic application of inhalable composites containing MNPs using a physiologically relevant metastatic triple negative breast cancer (TNBC) 3D model representative of the secondary lung malignancy characteristics (Fig. 5(A)).[93] The study evaluated the effect of both low and high MNP concentrations exposed to AMF of strength 691 Oe and 300 kHz for 1 h using a Taylor Winfield® AMF Source (Youngstown, OH). While the application of inhalable magnetic composites to the micrometastatic 3D TNBC model established from cancer and stromal cells showed no measurable harmful effects in the absence of AMF exposure, spheroids subjected to MHCT in the presence of higher MNP concentration (1 mg mL^{-1}) caused a significant increase in cellular death/damage with cellular disintegration and cellular debris release. Thus, indicating the therapeutic potential of these inhalable magnetic composites as a promising approach for the thermal treatment of diseased lungs.

A study by Ullah *et al.* (2019) evaluated macrophages as transporters for nanoparticle-conjugated drugs as well as controlled release by the simultaneous disruption of the cargo cells and the controlled AMF induced release of a toxin (maytansinoid), which was covalently linked to silica-coated SPIONs (T-SPIONs) *via* a thermo-sensitive linker in 3D tumor spheroids (Fig. 6(B)).[94] The 3D co-culture model was designed using T-SPION-loaded macrophages (J774a.1) : endothelial tumour cells (K-ECs) in a ratio of 1 : 40. The 3D cultures were exposed to AMF of strength 60 Oe and 779 kHz for 40 min using a magnetic field inductor Hu5000+ (Himmel, Germany). The results showed a strong reduction in cellular metabolic activity and thus viability in spheroids containing T-SPION-loaded macrophages after AMF application, indicating that the successful release of the toxin in the 3D spheroids induces death of the tumor cells.

A study further investigated the comparative therapeutic response of the mitochondrial-guiding agent triarylphosphonium (TPP)-conjugated MNPs (TPP-SPIONs) on liver tumor HepG2 cell viability when grown as monolayers and spheroids generated by co-culturing with 3T3 fibroblasts cells (Fig. 6(C)).[95] The results showed that TPP-SPIONs-mediated

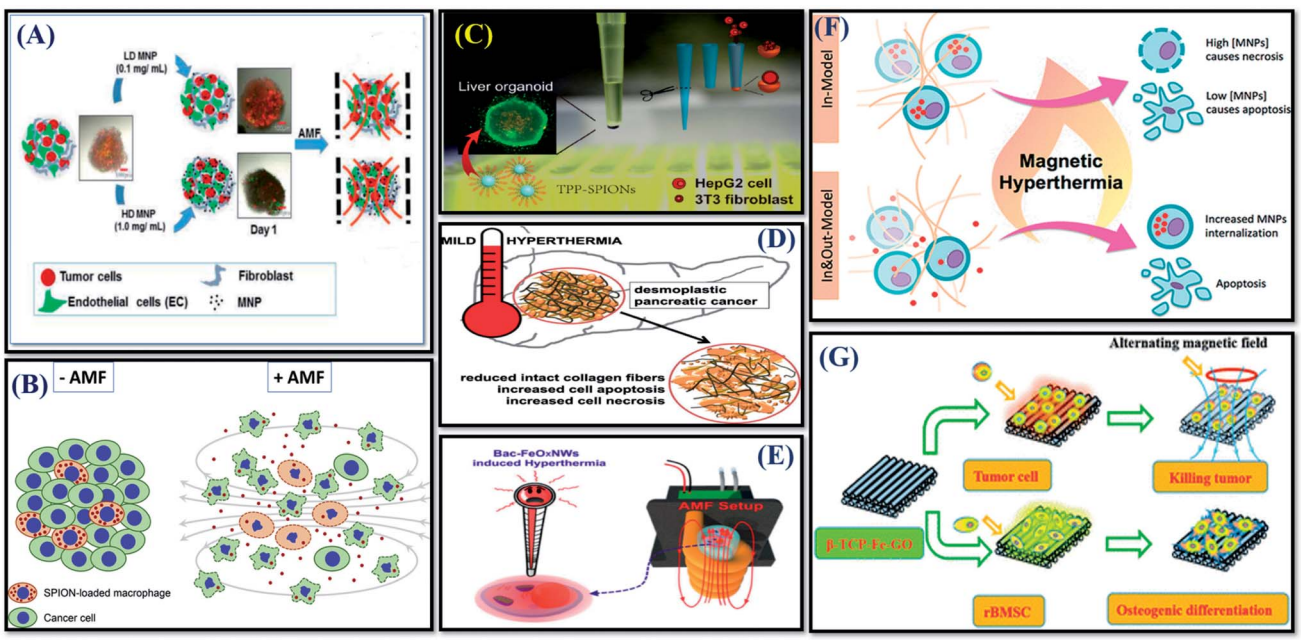

Fig. 6 Successful implications of 3D tumor cell culture models for MHCT-based therapies in tumor spheroids (A–D); and scaffolds (E–G). (A) Reprinted with permission from ref. 93 © (2017) Elsevier. (B) Reprinted with permission from ref. 94 © (2019) Elsevier. (C) Reprinted with permission from ref. 95 © (2019) American Chemical Society. (D) Reprinted with permission from ref. 96 © (2020) Elsevier. (E) Reprinted with permission from ref. 111 © (2016) American Chemical Society. (F) Reprinted with permission from ref. 112 © (2018) American Chemical Society. (G) With permission from ref. 113 © 2016 Royal Society of Chemistry.

MHCT is more efficient in reducing the HepG2 tumor cells viability in monolayers in contrast to co-cultured with stromal cells in 3D. During spheroid formation, the participating cells were observed to self-organize into a layered structure with HepG2 cells forming the core and 3T3 fibroblasts forming an outer shell. The presence of fibroblasts cells on the outer layer hindered SPIONs permeability inside the inner core of the spheroids owing to the cellular secretases (ECM proteins) by 3T3 cells. The employed liver tumor spheroid model represented the incapability of TPP-SPIONs to cause any significant difference in 3D cultures similar to tumor tissues *in vivo*, where the efficiency of TPP-SPIONs in MHCT treatment is inhibited by the ECM barrier. Thus, the study further validates the importance to consider the TME (as discussed in Section 2.1) to predict the true credibility of theranostic agents to be employed for MHCT. On similar lines, recently another study by Piehler *et al.*, also studied the therapeutic response of MHCT on fibrillary collagen architecture in *in vitro* pancreatic cancer model, comprising 3D heterotumor spheroids made up of pancreatic cancer (Panc-1) cells and fibroblasts (WI-38) cells, capable of producing collagen fibers (Fig. 6(D)).[96] Their results showed that besides activation of apoptotic cell death, such MNPs-based MHCT is conducive to leakages in the fibrillary collagen matrix and the pancreatic tumor tissue, which would further favor the blood perfusion and therefore enhance the permeation of therapeutic agents to the pancreatic tumors. This means that in non-accessible tumors, MHCT might induce irreversible damage to tumor ECM, improving the accessibility of tumors to the chemotherapeutic agents for effective adjuvant therapy.

3.2 Cell culture inserts

The cell culture inserts form the scaffold-based 3D systems in which cells grow anchored to biomaterials (like collagen, chitosan, gelatin, *etc.*) that resemble the ECM architecture.[50,97] For central nervous system therapies, the intact blood–brain barrier (BBB) constitutes a major roadblock for drug delivery, as 98% of small molecules are unable to enter the brain.[98,99] Strategies to enhance delivery have included either modifications of therapeutic agents, exploiting receptor-mediated transport systems, or temporary disruption of the BBB.[100] Development of new effective CNS therapies or delivery techniques requires a detailed understanding of the mechanisms of BBB transport, as well as extensive testing and optimization in model systems. One such most widely used *in vitro* model system for BBB research is the transwell assay, with applications in drug screening and mechanistic studies of BBB regulation.[101–103]

Numerous studies have demonstrated the therapeutic response of hyperthermia in combination with chemotherapy to aid the transport of drug-loaded nano-heaters across the BBB by temporarily impairing the permeability of the barrier and hence enhancing the amount of drug delivered at the desired tumor site, also maximizing the therapeutic efficiency of the hyperthermia approach.[104–107] A study demonstrated AMF-induced enhanced permeation of FePt nanoparticles across the BBB using an *in vitro* transwell model made up of MDCKII cells seeded onto the inserts (Corning, USA) coated with 2% gelatin solution.[108] The inserts when exposed to magnetic hyperthermia using an induction heating unit (Easy Heat 8310, Ambrell; UK) at 265 kHz for 5 min resulted in enhanced permeation of MNPs across the BBB attributed to the disruption of tight junctions by AMF exposure. Hence, indicating that MHCT not only significantly enhances the permeation of chemotherapeutic agents but may also increase the MNP BBB association and flux in the brain tumor tissues. Enhanced accumulation of hyperthermic agents in brain tissues will ultimately augment the effectiveness of MHCT-based brain therapies.

3.3 Scaffolds

Though the tumor spheroids generated mimic tumors under *in vivo* conditions, they still fail to mimic the tumor microenvironment completely as they generally lack the presence of ECM.[10] ECM comprising components like collagen fibers, hyaluronan, glycoproteins and proteoglycans plays a crucial role in the cellular microenvironment as it holds the cells together, enabling them to form complex tissues.[109] For the cancer cells to metastasize, they need to disrupt the ECM structure to generate space for further advancement of the malignant cells.[109,110] Hence, while evaluating the true therapeutic response of MHCT in cell culture models, consideration of ECM surfaces as an essential parameter.

A study by Kumeria *et al.*, demonstrated the application of doxorubicin-loaded iron oxide nanowires produced from bacteria – *Mariprofundus ferrooxydans* (Bac-FeO_xNWs) as hyperthermic agents for 3D cultures of human breast cancer cells (MDA-MB231-TXSA) developed in Matrigel (Fig. 6(E)).[111] The AMF application (using a custom-built AMF generator operating at 230 kHz) increased the localized temperature by 14 °C with ~34% reduction in cell viability. Another study reported the evaluation of cellular damage mechanisms by MHCT by generating collagen-based 3D cell culture tumor models using murine macrophage/monocyte cell line (RAW 264.7) (Fig. 6(F)).[112] Collagen forms the most abundant protein of the extracellular matrix and is also known to play a crucial role in the tumor ECM. Activation of cell death mechanisms was observed on exposure of 3D cell cultures to an AMF of strength 377.5 kHz and field amplitude of 13 kA m^{-1} using a commercial AMF generator (nB nanoscale Biomagnetics, Spain). Also, the collagen matrix was observed to be altered by extracellular MNPs indicating use of magnetic hyperthermia as a tool to disrupt the TME and improve the effectiveness of other cancer treatments that have limitations in crossing this barrier.

Further, a study reported the development of a 3D-printed b-tricalcium phosphate bioceramic scaffold with surface modification of Fe_3O_4 nanoparticles/graphene oxide nanocomposite layers (b-TCP–Fe–GO) for bone tumor therapy (Fig. 6(G)).[113] The scaffolds exhibited magnetothermal properties owing to the Fe_3O_4 nanoparticles in the scaffolds with temperature rise up to 50–80 °C under AMF exposure for 15 minutes using a DM100 system (nB nanoscale Biomagnetics, Spain). The excellent magnetothermal effect of b-TCP–Fe–GO scaffolds induced more than 75% cell death for osteosarcoma cells (MG-63). Thus, indicating the potential application of such magneto-active scaffolds for cancer therapy.

Table 3 Properties of 2D (monolayers) and 3D (spheroids, inserts, scaffolds and microfluidic chips) *in vitro* tumor models

Cell culture models	TME resemblance	Cellular properties	Possible roles in the MHCT study	MHCT study parameters	Ref.
2D cultures monolayers - cells cultured on rigid and flat surfaces, typically made of glass and polystyrene 	***Low***: cells display undetectable to low expression of ECM proteins like collagen. Exhibit poor cell–cell and cell–ECM contacts	***Heterogeneity***: uniform. Cells are subject to uniform distribution of nutrients and growth conditions ***Gene expression***: generally lower than that observed in tumor tissues	Initial nanoparticle or drug efficacy studies either alone or in combination with MHCT	***Cell viability***: analyzed by various techniques like - ***Quantitative measurement***: MTT, alamar blue, XTT, flow cytometry ***Qualitative measurement***: live/dead assay; tunnel assay	14 and 15
		Drug gradient: no drug gradient is observed indicating uniform effect of drugs administered giving higher cell death		***Heat shock response***: expression studies of HSPs on heat stress and enhancement of the therapeutic effect on knockdown of HSPs using siRNA	85
		Absence of drug penetration barriers.		***Combinatorial studies***: effect of MHCT in combination with other adjuvant therapies like chemotherapy and radiation therapy	1 and 14
3D cultures: spheroids – aggregates or clusters of cells 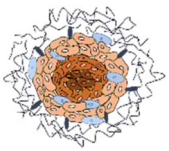	***Moderate to high***: ECM is generated in a similar fashion as in *in vivo* conditions. Exhibit higher cell–cell and cell–ECM contacts	***Heterogeneity***: non-uniform. Cells gets spontaneously organized into different layers (proliferation zone, quiescent zone and necrotic zone) mimicking *in vivo* conditions	Nanoparticles penetration depth in the tumors – forming nanoparticle gradient in different cellular layers	***Cell viability***: analyzed by various techniques like-quantitative measurement: alamar blue, lactate dehydrogenase, acid phosphatase, flow cytometry	111, 113 and 122
		Gene expression: differential gene expression is observed among cells present in different layers of the tumor cell culture models. Overall, higher expression of genes is observed as compared to 2D cultures that are similar to those observed in tumor tissues	Therapeutic gradient formed due to increased central necrotic zone on AMF exposure with outer cells being not much affected	***Qualitative measurement***: live/dead assay; tunnel assay	
		Drug gradient: existence of drug gradient is observed as layered cell organization in 3D cultures results in hindrance to free penetration of drugs/ nanomaterials administrated to the centrally present cells (necrotic zone). Drug penetration barriers formed by ECM components and cellular organization are present		***Heat shock response***: differential expression of HSPs as compared to 2D cultures	74 and 80
Inserts - cells grown on scaffold-based biomaterials 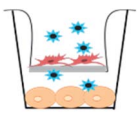	3D scaffolds in the inserts may be constructed using ECM mimicking biomaterials like collagen, fibronectin, *etc.* Exhibit higher cell–cell and cell–ECM contacts		Nanoparticle flux across the biological barriers by temporarily disruption of the tight junctions by AMF exposure	***TME***: importance of the TME in limiting drug/MNP penetration inside 3D cultures. Degradation of ECM proteins on AMF application	95, 96 and 112
Scaffolds - cells seeded in gel-based 3D structures 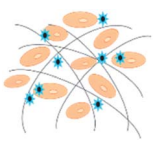	Cells are normally embedded in biomaterials that resemble properties of ECM proteins. Exhibit higher cell–cell and cell–ECM contacts		Effect of AMF exposure at different tumor stages by varying the scaffold architecture	***Tumor penetration***: effect of AMF application in enhanced penetration of nanoparticles in the 3D tumor cultures either by ECM degradation or temporary barrier disruption	96 and 112
			Effect of MHCT on cellular processes when shielded by ECM-like environment	***Combinatorial studies***: effect of MHCT in combination with other adjuvant therapies like chemotherapy and radiation therapy	57

Table 3 (*Contd.*)

Cell culture models	TME resemblance	Cellular properties	Possible roles in the MHCT study	MHCT study parameters	Ref.
Microfluidic devices - cells seeded in organon chips 	Surfaces of the chips are coated with biomaterials resembling ECM like collagen, fibronectin, *etc.* Exhibit higher cell–cell and cell–ECM contacts		Study of AMF effects under physiological mimicking flow rates and cellular environment		

3.4 Microfluidic devices

Microfluidics has helped tremendously to understand the biological processes involved for greater development in various fields like immunoassays,[114] DNA analyses,[115] drug assays,[116] tissue engineering,[117] biosensors,[118] *etc.* Among all the 3D culture techniques, the microfluidic platform is one of the most promising methods, as the system reproduces cell–cell interactions, growth factor gradients, and mechanical and shear stress properties of the TME with a high level of accuracy compared to other methods, thus replacing and reducing the use of murine models for several biomedical applications.[119–121] One such use of these therapies is applied by hyperthermia treatments, such as MHT in tumors.

The efficacy of MHCT on an organ-on-a-chip designed for a glioblastoma model has also been evaluated to mimic tumors by Mamani *et al.*[122] In order to generate the GBM tumor model, they cultured rat glioma C6 cells in a microfluidic device from SynVivo Inc (Huntsville, AL, US). On administration of aminosilane-coated MNPs (10 mg_{Fe} mL^{-1}), cells were exposed to AMF of strength 300 Oe and 305 kHz for a period of 30 min using a DMC1-equipped DM100 nanomagnetic heating system (nB nanoScale Biomagnetics, Spain). The study validated the therapeutic process of MHCT in the GBM on-a-chip tumor model to be effective as it resulted in complete cell lyses after 30 minutes of AMF exposure.

As far as our knowledge is concerned, until now, this is the only study reported that demonstrates the application of MHCT in *in vitro* 3D cultures established in a microfluidic device. However, this study paves way for more research into the area *in lieu* of bridging the gap between successful therapeutic response from *in vitro* to *in vivo* conditions owing to the feasibility and reproducibility of the cultures.

Table 3 lists and compares the properties and study design parameters investigated and also the possible roles of the tumor models for both 2D (monolayers) and 3D (spheroids, inserts, scaffolds and microfluidic chips) cell cultures for MHCT.

4. Concluding remarks and future prospects

Even though evaluating therapeutic responses in 3D *in vitro* models can enhance the probability of achieving an optimized response in human patients under clinical trials for magnetic hyperthermia; only limited investigation in 3D models have been performed to date. Designing 3D *in vitro* tumor models would aid researchers to conduct rapid experiments on the ways of cancer progression and development at a lower cost with limited requirement of *in vivo* animal models. Optimization of MHCT based experimental parameters (frequency and magnitude of the magnetic field applied), investigation of penetration depth and distribution profile of MNPs inside the solid tumors, bio-availability window of these injected MNPs at the tumor site, feasibility of re-application of AMF to enhance the therapeutic outcome, the extent of mechanical damage or the cellular stress caused to cells arranged in all the three layers (dividing, senescent and necrotic) of spheroid cultures, monitoring re-growth of tumors on re-culturing after AMF exposure and in-depth analysis of signal transduction pathways responsible for both cell death and the acquired thermotolerance in 3D cultures can widely aid in establishing MHCT as the desired treatment regime for cancer therapy. Also, magnetic hyperthermia treatment could be done with fewer casualties and it could be more effective and more accurate as per the patient requirements.

Another important aspect is the personalized medicine, which by using 3D culturing techniques, researchers could alter cellular components like expression of certain growth factors or surface receptors; insertion and/or deletion of specific gene sequences in the cells, thus mimicking the individual features of patient's tumors to better predict the molecular events associated with the tumor pathogenesis. Such a true replica of the tumor progression cascade could further augment the *in vitro* optimization process of MHCT, enhancing its therapeutic outcome.

Further, evaluation of scaffolds like hydrogels with varying crosslinking degree could help in tailoring 3D structures with different mechanical properties that could resemble different stages of tumor development. Thus, investigation of MHCT in such cultures could give a better idea of how cancer cells might respond or progress after AMF exposure at different stages of cancer. The analyses of therapeutic responses in such *in vitro* MHCT models may also give a clear picture of the salient aspects of *in vivo* neoplasm growth, investigation of oncogene expression, and better reflect the invasive nature of the malignant tissues. Thus, this constitutes a starting point for future work on developing 3D *in vitro* tumor models for therapeutic and diagnostic impact of MHCT against advanced stage malignancies.

Author contributions

Ruby Gupta – drafting of the manuscript, literature search and compilation of the data. Deepika Sharma – contributed towards drafting and final editing of the manuscript.

Conflicts of interest

There are no conflicts to declare.

Acknowledgements

The work was financially supported by Department of Science and Technology – Science and Engineering Research Board grant [ECR/2017/000049]. The authors also acknowledge the support by Institute of Nano Science and Technology, Mohali.

References

1 R. Gupta and D. Sharma, Evolution of magnetic hyperthermia for glioblastoma multiforme therapy, *ACS Chem. Neurosci.*, 2019, **10**, 1157–1172, DOI: 10.1021/acschemneuro.8b00652.

2 N. R. Datta, S. Krishnan, D. E. Speiser, E. Neufeld, N. Kuster, S. Bodis and H. Hofmann, Magnetic nanoparticle-induced hyperthermia with appropriate payloads: Paul Ehrlich's "magic (nano)bullet" for cancer theranostics?, *Cancer Treat. Rev.*, 2016, **50**, 217–227, DOI: 10.1016/j.ctrv.2016.09.016.

3 X. Liu, Y. Zhang, Y. Wang, W. Zhu, G. Li, X. Ma, Y. Zhang, S. Chen, S. Tiwari, K. Shi, S. Zhang, H. M. Fan, Y. X. Zhao and X. J. Liang, Comprehensive understanding of magnetic hyperthermia for improving antitumor therapeutic efficacy, *Theranostics*, 2020, **10**, 3793–3815, DOI: 10.7150/thno.40805.

4 R. K. Gilchrist, R. Medal, W. D. Shorey, R. C. Hanselman, J. C. Parrott and C. B. Taylor, Selective inductive heating of lymph nodes, *Ann. Surg.*, 1957, **146**, 596–606, DOI: 10.1097/00000658-195710000-00007.

5 B. Thiesen and A. Jordan, Clinical applications of magnetic nanoparticles for hyperthermia, *Int. J. Hyperthermia*, 2008, **24**, 467–474, DOI: 10.1080/02656730802104757.

6 R. Kumar, A. Chauhan and B. K. Kuanr, A robust *in vitro* anticancer activity *via* magnetic hyperthermia mediated by colloidally stabilized mesoporous silica encapsulated $La_{0.7}Sr_{0.3}MnO_3$ core-shell structure, *Colloids Surf., A*, 2021, **615**, 126212, DOI: 10.1016/j.colsurfa.2021.126212.

7 D. Nieciecka, J. Celej, M. Żuk, A. Majkowska-Pilip, K. Żelechowska-Matysiak, A. Lis and M. Osial, Hybrid system for local drug delivery and magnetic hyperthermia based on SPIONs loaded with doxorubicin and epirubicin, *Pharmaceutics*, 2021, **13**, 480, DOI: 10.3390/pharmaceutics13040480.

8 J. Sánchez, M. Rodríguez-Reyes, D. A. Cortés-Hernández, C. A. Ávila-Orta and P. Y. Reyes-Rodríguez, Heating capacity and biocompatibility of Pluronic-coated manganese gallium ferrites for magnetic hyperthermia treatment, *Colloids Surf., A*, 2020, **612**, 125986, DOI: 10.1016/j.colsurfa.2020.125986.

9 Z. Hedayatnasab, A. Dabbagh, F. Abnisa and W. M. A. Wan Daud, Polycaprolactone-coated superparamagnetic iron oxide nanoparticles for *in vitro* magnetic hyperthermia therapy of cancer, *Eur. Polym. J.*, 2020, **133**, 109789, DOI: 10.1016/j.eurpolymj.2020.109789.

10 G. N. A. Rego, M. P. Nucci, J. B. Mamani, F. A. Oliveira, L. C. Marti, I. S. Filgueiras, J. M. Ferreira, C. C. Real, D. dP. Faria, P. L. Espinha, D. M. C. Fantacini, L. E. B. Souza, D. T. Covas, C. A. Buchpiguel and L. F. Gamarra, Therapeutic efficiency of multiple applications of magnetic hyperthermia technique in glioblastoma using aminosilane coated iron oxide nanoparticles: *in vitro* and *in vivo* study, *Int. J. Mol. Sci.*, 2020, **21**, 958, DOI: 10.3390/ijms21030958.

11 M. Soleymani, S. Khalighfard, S. Khodayari, H. Khodayari, M. R. Kalhori, M. R. Hadjighassem, Z. Shaterabadi and A. M. Alizadeh, Effects of multiple injections on the efficacy and cytotoxicity of folate-targeted magnetite nanoparticles as theranostic agents for MRI detection and magnetic hyperthermia therapy of tumor cells, *Sci. Rep.*, 2020, **10**, 1695, DOI: 10.1038/s41598-020-58605-3.

12 A. L. Ramirez-Nuñez, L. F. Jimenez-Garcia, G. F. Goya, B. Sanz and J. Santoyo-Salazar, *In vitro* magnetic hyperthermia using polyphenol-coated Fe_3O_4@γFe_2O_3 nanoparticles from Cinnamomun verum and Vanilla planifolia: the concert of green synthesis and therapeutic possibilities, *Nanotechnology*, 2018, **29**, 074001, DOI: 10.1088/1361-6528/aaa2c1.

13 S. E. Minaei, S. Khoei, S. Khoee, F. Vafashoar and V. P. Mahabadi, *In vitro* anti-cancer efficacy of multi-functionalized magnetite nanoparticles combining alternating magnetic hyperthermia in glioblastoma cancer cells, *Mater. Sci. Eng., C*, 2019, **101**, 575–587, DOI: 10.1016/j.msec.2019.04.007.

14 R. Gupta and D. Sharma, Manganese-doped magnetic nanoclusters for hyperthermia and photothermal glioblastoma therapy, *ACS Appl. Nano Mater.*, 2020, **3**, 2026–2037, DOI: 10.1021/acsanm.0c00121.

15 R. Gupta and D. Sharma, Biofunctionalization of magnetite nanoparticles with stevioside: effect on the size and thermal behaviour for use in hyperthermia applications, *Int. J. Hyperthermia*, 2019, **36**, 302–312, DOI: 10.1080/02656736.2019.1565787.

16 R. M. Patil, N. D. Thorat, P. B. Shete, S. V. Otari, B. M. Tiwale and S. H. Pawar, *In vitro* hyperthermia with improved colloidal stability and enhanced SAR of magnetic core/shell nanostructures, *Mater. Sci. Eng., C*, 2016, **59**, 702–709, DOI: 10.1016/j.msec.2015.10.064.

17 Y. Oh, N. Lee, H. W. Kang and J. Oh, *In vitro* study on apoptotic cell death by effective magnetic hyperthermia with chitosan-coated $MnFe_2O_4$, *Nanotechnology*, 2016, **27**, 115101, DOI: 10.1088/0957-4484/27/11/115101.

18 Y. Iqbal, H. Bae, I. Rhee and S. Hong, Control of the saturation temperature in magnetic heating by using polyethylene-glycol-coated rod-shaped nickel-ferrite

($NiFe_2O_4$) nanoparticles, *J. Korean Phys. Soc.*, 2016, **68**, 587–592, DOI: 10.3938/jkps.68.587.

19 B. B. Lahiri, T. Muthukumaran and J. Philip, Magnetic hyperthermia in phosphate coated iron oxide nanofluids, *J. Magn. Magn. Mater.*, 2016, **407**, 101–113, DOI: 10.1016/jjmmm201601044.

20 Y. Iqbal, H. Bae, I. Rhee and S. Hong, Magnetic heating of silica-coated manganese ferrite nanoparticles, *J. Magn. Magn. Mater.*, 2016, **409**, 80–86, DOI: 10.1016/jjmmm201602078.

21 A. Hanini, L. Lartigue, J. Gavard, K. Kacem, C. Wilhelm, F. Gazeau, F. Chau and S. Ammar, Zinc substituted ferrite nanoparticles with $Zn_{0.9}Fe_{2.1}O_4$ formula used as heating agents for *in vitro* hyperthermia assay on glioma cells, *J. Magn. Magn. Mater.*, 2016, **416**, 315–320, DOI: 10.1016/j.jmmm.2016.05.016.

22 H. Chiriac, T. Petreus, E. Carasevici, L. Labusca, D.-D. Herea, C. Danceanu and N. Lupu, *In vitro* cytotoxicity of Fe–Cr–Nb–B magnetic nanoparticles under high frequency electromagnetic field, *J. Magn. Magn. Mater.*, 2015, **380**, 13–19, DOI: 10.1016/j.jmmm.2014.10.015.

23 E. Fantechi, C. Innocenti, M. Albino, E. Lottini and C. Sangregorio, Influence of cobalt doping on the hyperthermic efficiency of magnetite nanoparticles, *J. Magn. Magn. Mater.*, 2015, **380**, 365–371, DOI: 10.1016/j.jmmm.2014.10.082.

24 E. Garaio, J. M. Collantes, J. A. Garcia, F. Plazaola, S. Mornet, F. Couillaud and O. Sandre, A wide-frequency range ACmagnetometer tomeasure the specific absorption rate in nanoparticles for magnetic hyperthermia, *J. Magn. Magn. Mater.*, 2014, **368**, 432–437, DOI: 10.1016/j.jmmm.2013.11.021.

25 P. B. Shete, R. M. Patil, N. D. Thorat, A. Prasad, R. S. Ningthoujam, S. J. Ghosh and S. H. Pawar, Magnetic chitosan nanocomposite for hyperthermia therapy application: preparation, characterization and *in vitro* experiments, *Appl. Surf. Sci.*, 2014, **288**, 149–157, DOI: 10.1016/j.apsusc.2013.09.169.

26 V. M. Khot, A. B. Salunkhe, N. D. Thorat, R. S. Ningthoujam and S. H. Pawar, Induction heating studies of dextran coated mgfe2o4 nanoparticles for magnetic hyperthermia, *Dalton Trans.*, 2013, **42**, 1249–1258, DOI: 10.1039/C2DT31114C.

27 N. D. Thorat, R. M. Patil, V. M. Khot, A. B. Salunkhe, A. I. Prasad, K. C. Barick, R. S. Ningthoujam and S. H. Pawar, Highly water-dispersible surface-functionalized lsmo nanoparticles for magnetic fluid hyperthermia application, *New J. Chem.*, 2013, **37**, 2733, DOI: 10.1039/C3NJ00007A.

28 S. Laurent, S. Dutz, U. O. Hafeli and M. Mahmoudide, Magnetic fluid hyperthermia: focus on superparamagnetic iron oxide nanoparticles, *Adv. Colloid Interface Sci.*, 2011, **166**, 8–23, DOI: 10.1016/j.cis.2011.04.003.

29 M. Wang, J. Zhao, L. Zhang, F. Wei, Y. Lian, Y. Wu, Z. Gong, S. Zhang, J. Zhou, K. Cao, X. Li, W. Xiong, G. Li, Z. Zeng and C. Guo, Role of tumor microenvironment in tumorigenesis, *J. Cancer*, 2017, **8**, 761–773, DOI: 10.7150/jca.17648.

30 B. R. da Cunha, C. Domingos, A. C. B. Stefanini, T. Henrique, G. M. Polachini, P. Castelo-Branco and E. H. Tajara, Cellular Interactions in the Tumor Microenvironment: The Role of Secretome, *J. Cancer*, 2019, **10**, 4574–4587, DOI: 10.7150/jca.21780.

31 M. De Palma, D. Biziato and T. V. Petrova, Microenvironmental regulation of tumour angiogenesis, *Nat. Rev. Cancer*, 2017, **17**, 457–474, DOI: 10.1038/nrc.2017.51.

32 B. Lim, W. A. Woodward, X. Wang, J. M. Reuben and N. T. Ueno, Inflammatory breast cancer biology: the tumour microenvironment is key, *Nat. Rev. Cancer*, 2018, **8**, 485–499, DOI: 10.1038/s41568-018-0010-y.

33 K. M. Yamada and E. Cukierman, Modeling tissue morphogenesis and cancer in 3D, *Cell*, 2007, **130**, 601–610, DOI: 10.1016/j.cell.2007.08.006.

34 K. Duval, H. Grover, L. H. Han, Y. Mou, A. F. Pegoraro, J. Fredberg and Z. Chen, Modeling Physiological Events in 2D *vs.* 3D Cell Culture, *Physiology*, 2017, **32**, 266–277, DOI: 10.1152/physiol.00036.2016.

35 J. Hoarau-Véchot, A. Rafii, C. Touboul and J. Pasquier, Halfway between 2D and Animal Models: Are 3D Cultures the Ideal Tool to Study Cancer-Microenvironment Interactions?, *Int. J. Mol. Sci.*, 2018, **19**, 181, DOI: 10.3390/ijms19010181.

36 M. Cekanova and K. Rathore, Animal models and therapeutic molecular targets of cancer: utility and limitations, *Drug Des., Dev. Ther.*, 2014, **8**, 1911–1921, DOI: 10.2147/DDDT.S49584.

37 T. Voskoglou-Nomikos, J. L. Pater and L. Seymour, Clinical predictive value of the *in vitro* cell line, human xenograft, and mouse allograft preclinical cancer models, *Clin. Cancer Res.*, 2003, **9**, 4227–4239.

38 I. W. Mak, N. Evaniew and M. Ghert, Lost in translation: animal models and clinical trials in cancer treatment, *Am. J. Transl. Res.*, 2014, **6**, 114–118.

39 K. Klinghammer, W. Walther and J. Hoffmann, Choosing wisely - Preclinical test models in the era of precision medicine, *Cancer Treat. Rev.*, 2017, **55**, 36–45, DOI: 10.1016/j.ctrv.2017.02.009.

40 C. Dubessy, J. L. Merlin, C. Marchal and F. Guillemince, Spheroids in radiobiology and photodynamic therapy, *Critical Rev. Oncol.*, 2000, **36**, 179–192, DOI: 10.1016/S1040-8428(00)00085-8.

41 A. Riedl, M. Schlederer, K. Pudelko, M. Stadler, S. Walter, D. Unterleuthner, C. Unger, N. Kramer, M. Hengstschläger, L. Kenner, D. Pfeiffer, G. Krupitza and H. Dolznig, Comparison of cancer cells in 2D *vs.* 3D culture reveals differences in AKT-mTOR-S6K signaling and drug responses, *J. Cell Sci.*, 2017, **130**, 203–218, DOI: 10.1242/jcs.188102.

42 S. C. Brüningk, I. Rivens, C. Box, U. Oelfke and G. ter Haar, 3D tumour spheroids for the prediction of the effects of radiation and hyperthermia treatments, *Sci. Rep.*, 2020, **10**, 1653, DOI: 10.1038/s41598-020-58569-4.

43 S. Breslin and L. O'Driscoll, Three-dimensional cell culture: the missing link in drug discovery, *Drug Discovery Today*, 2013, **18**, 240–249, DOI: 10.1016/j.drudis.2012.10.003.

44 E. Fennema, N. Rivron, J. Rouwkema, C. van Blitterswijk and J. Boer, Spheroid culture as a tool for creating 3D complex tissues, *Trends Biotechnol.*, 2013, **31**, 108–115, DOI: 10.1016/j.tibtech.2012.12.003.

45 M. Zimmermann, C. Box and S. A. Eccles, Two-dimensional *vs.* three-dimensional *in vitro* tumor migration and invasion assays, *Methods Mol. Biol.*, 2013, **986**, 227–252, DOI: 10.1007/978-1-62703-311-4_15.

46 K. Pietras and A. Ostman, Hallmarks of cancer: interactions with the tumor stroma, *Exp. Cell Res.*, 2010, **316**, 1324–1331, DOI: 10.1016/j.yexcr.2010.02.045.

47 D. W. McMillin, J. M. Negri and C. S. Mitsiades, The role of tumour-stromal interactions in modifying drug response: challenges and opportunities, *Nat. Rev. Drug Discovery*, 2013, **12**, 217–228, DOI: 10.1038/nrd3870.

48 T. D. Tlsty and L. M. Coussens, Tumor stroma and regulation of cancer development, *Annu. Rev. Pathol.: Mech. Dis.*, 2006, **1**, 119–150, DOI: 10.1146/annurev.pathol.1.110304.100224.

49 D. S. Tan, R. Agarwal and S. B. Kaye, Mechanisms of transcoelomic metastasis in ovarian cancer, *Lancet Oncol.*, 2006, **7**, 925–934, DOI: 10.1016/S1470-2045(06)70939-1.

50 E. C. Costa, A. F. Moreira, D. de Melo-Diogo, V. M. Gaspar, M. P. Carvalho and I. J. Correia, 3D tumor spheroids: an overview on the tools and techniques used for their analysis, *Biotechnol. Adv.*, 2016, **34**, 1427–1441, DOI: 10.1016/j.biotechadv.2016.11.002.

51 W. H. Koppenol, P. L. Bounds and C. V. Dang, Otto Warburg's contributions to current concepts of cancer metabolism, *Nat. Rev. Cancer*, 2011, **11**, 325–337, DOI: 10.1038/nrc3038.

52 O. Trédan, C. M. Galmarini, K. Patel and I. F. Tannock, Drug resistance and the solid tumor microenvironment, *J. Natl. Cancer Inst.*, 2007, **99**, 1441–1454, DOI: 10.1093/jnci/djm135.

53 A. S. Nunes, A. S. Barros, E. C. Costa, A. F. Moreira and I. J. Correia, 3D tumor spheroids as *in vitro* models to mimic *in vivo* human solid tumors resistance to therapeutic drugs, *Biotechnol. Bioeng.*, 2019, **116**, 206–226, DOI: 10.1002/bit.26845.

54 G. M. Hahn, Metabolic aspects of the role of hyperthermia in mammalian cell inactivation and their possible relevance to cancer treatment, *Cancer Res.*, 1974, **34**, 3117–3123.

55 R. Sutherland and W. Macfarlane, Cytotoxicity of radiosensitizers in multicell spheroids: combination treatment with hyperthermia, *Br. J. Cancer*, 1978, **37**, 168.

56 A. Ostman and M. Augsten, Cancer-associated fibroblasts and tumor growth – bystanders turning into key players, *Curr. Opin. Genet. Dev.*, 2009, **19**, 67–73, DOI: 10.1016/j.gde.2009.01.003.

57 Y. L. Su, J. H. Fang, C. Y. Liao, C. T. Lin, Y. T. Li and S. H. Hu, Targeted mesoporous iron oxide nanoparticles-encapsulated perfluorohexane and a hydrophobic drug for deep tumor penetration and therapy, *Theranostics*, 2015, **5**, 1233–1248, DOI: 10.7150/thno.12843.

58 S. Yamamoto, M. Okochi, K. Jimbow and H. Honda, Three-dimensional magnetic cell array for evaluation of anti-proliferative effects of chemo-thermo treatment on cancer spheroids, *Biotechnol. Bioprocess Eng.*, 2015, **20**, 488–497, DOI: 10.1007/s12257-014-0724-y.

59 A. L. Correia and M. J. Bissell, The tumor microenvironment is a dominant force in multidrug resistance, *Drug Resist. Updates*, 2012, **15**, 39–49, DOI: 10.1016/j.drup.2012.01.006.

60 P. Lu, V. M. Weaver and Z. Werb, The extracellular matrix: a dynamic niche in cancer progression, *J. Cell Biol.*, 2012, **196**, 395–406, DOI: 10.1083/jcb.201102147.

61 M. van Dijk, S. A. Göransson and S. Strömblad, Cell to extracellular matrix interactions and their reciprocal nature in cancer, *Exp. Cell Res.*, 2013, **319**, 1663–1670, DOI: 10.1016/j.yexcr.2013.02.006.

62 L. Seguin, J. S. Desgrosellier, S. M. Weis and D. A. Cheresh, Integrins and cancer: regulators of cancer stemness, metastasis, and drug resistance, *Trends Cell Biol.*, 2015, **25**, 234–240, DOI: 10.1016/j.tcb.2014.12.006.

63 H. Hamidi and J. Ivaska, Every step of the way: integrins in cancer progression and metastasis, *Nat. Rev. Cancer*, 2018, **18**, 533–548, DOI: 10.1038/s41568-018-0038-z.

64 G. A. Howe and C. L. Addison, β1 integrin: an emerging player in the modulation of tumorigenesis and response to therapy, *Cell Adhes. Migr.*, 2012, **6**, 71–77, DOI: 10.4161/cam.20077.

65 H. L. Goel, J. M. Underwood, J. A. Nickerson, C. C. Hsieh and L. R. Languino, Beta1 integrins mediate cell proliferation in three-dimensional cultures by regulating expression of the sonic hedgehog effector protein, GLI1, *J. Cell. Physiol.*, 2010, **224**, 210–217, DOI: 10.1002/jcp.22116.

66 S. Ghosh, G. C. Spagnoli, I. Martin, S. Ploegert, P. Demougin, M. Heberer and A. Reschner, Three-dimensional culture of melanoma cells profoundly affects gene expression profile: a high density oligonucleotide array study, *J. Cell. Physiol.*, 2005, **204**, 522–531, DOI: 10.1002/jcp.20320.

67 H. R. Kumar, X. Zhong, D. J. Hoelz, F. J. Rescorla, R. J. Hickey, L. H. Malkas and J. A. Sandoval, Three-dimensional neuroblastoma cell culture: proteomic analysis between monolayer and multicellular tumor spheroids, *Pediatr. Surg. Int.*, 2008, **24**, 1229–1234, DOI: 10.1007/s00383-008-2245-2.

68 T. T. Chang and M. Hughes-Fulford, Monolayer and spheroid culture of human liver hepatocellular carcinoma cell line cells demonstrate distinct global gene expression patterns and functional phenotypes, *Tissue Eng., Part A*, 2009, **15**, 559–567, DOI: 10.1089/ten.tea.2007.0434.

69 H. Kim, Y. Phung and M. Ho, Changes in global gene expression associated with 3D structure of tumors: an ex vivo matrix-free mesothelioma spheroid model, *PLoS One*, 2012, **7**, e39556, DOI: 10.1371/journal.pone.0039556.

70 A. C. Luca, S. Mersch, R. Deenen, S. Schmidt, I. Messner, K. L. Schäfer, S. E. Baldus, W. Huckenbeck, R. P. Piekorz,

W. T. Knoefel, A. Krieg and N. H. Stoecklein, Impact of the 3D microenvironment on phenotype, gene expression, and EGFR inhibition of colorectal cancer cell lines, *PLoS One*, 2013, **8**, e59689, DOI: 10.1371/journal.pone.0059689.

71 C. Boudesco, S. Cause, G. Jego and C. Garrido, Hsp70: A Cancer Target Inside and Outside the Cell, *Methods Mol. Biol.*, 2018, **1709**, 371–396, DOI: 10.1007/978-1-4939-7477-1_27.

72 F. X. Beck, R. Grünbein, K. Lugmayr and W. Neuhofer, Heat shock proteins and the cellular response to osmotic stress, *Cell. Physiol. Biochem.*, 2000, **10**, 303–306, DOI: 10.1159/000016362.

73 C. H. Yeh, S. P. Hsu, C. C. Yang, C. T. Chien and N. P. Wang, Hypoxic preconditioning reinforces HIF-alpha-dependent HSP70 signaling to reduce ischemic renal failure-induced renal tubular apoptosis and autophagy, *Life Sci.*, 2010, **86**, 115–123, DOI: 10.1016/j.lfs.2009.11.022.

74 A. S. Song, A. M. Najjar and K. R. Diller, Thermally induced apoptosis, necrosis, and heat shock protein expression in 3D culture, *J. Biomech. Eng.*, 2014, **136**, 071006, DOI: 10.1115/1.4027272.

75 G. Multhoff, A. G. Pockley, T. E. Schmid and D. Schilling, The role of heat shock protein 70 (Hsp70) in radiation-induced immunomodulation, *Cancer Lett.*, 2015, **368**, 179–184, DOI: 10.1016/j.canlet.2015.02.013.

76 M. P. Collier and J. L. Benesch, Small heat-shock proteins and their role in mechanical stress, *Cell Stress Chaperones*, 2020, **25**, 601–613, DOI: 10.1007/s12192-020-01095-z.

77 K. R. Diller, Stress protein expression kinetics, *Annu. Rev. Biomed. Eng.*, 2006, **8**, 403–424, DOI: 10.1146/annurev.bioeng.7.060804.100449.

78 L. B. Sims, M. K. Huss, H. B. Frieboes and J. M. Steinbach-Rankins, Distribution of PLGA-modified nanoparticles in 3D cell culture models of hypo-vascularized tumor tissue, *J. Nanobiotechnol.*, 2017, **15**, 67, DOI: 10.1186/s12951-017-0298-x.

79 R. E. Durand, Effects of hyperthermia on the cycling, noncycling, and hypoxic cells of irradiated and unirradiated multicell spheroids, *Radiat. Res.*, 1978, **75**, 373–384.

80 J. Jakubowicz-Gil, R. Paduch, A. Gawron and M. Kandefer-Szerszeń, The effect of heat shock, cisplatin, etoposide and quercetin on Hsp27 expression in human normal and tumour cells, *Folia Histochem. Cytochem.*, 2002, **40**, 31–35.

81 S. K. Calderwood, M. A. Khaleque, D. B. Sawyer and D. R. Ciocca, Heat shock proteins in cancer: chaperones of tumorigenesis, *Trends Biochem. Sci.*, 2006, **31**, 164–172, DOI: 10.1016/j.tibs.2006.01.006.

82 J. Radons, The human HSP70 family of chaperones: where do we stand?, *Cell Stress Chaperones*, 2016, **21**, 379–404, DOI: 10.1007/s12192-016-0676-6.

83 A. Hoter, M. E. El-Sabban and H. Y. Naim, The HSP90 Family: Structure, Regulation, Function, and Implications in Health and Disease, *Int. J. Mol. Sci.*, 2018, **19**, 2560, DOI: 10.3390/ijms19092560.

84 B. J. Lang, M. E. Guerrero-Giménez, T. L. Prince, A. Ackerman, C. Bonorino and S. K. Calderwood, Heat shock proteins are essential components in transformation and tumor progression: Cancer cell intrinsic pathways and beyond, *Int. J. Mol. Sci.*, 2019, **20**, 4507, DOI: 10.3390/ijms20184507.

85 K. Sekihara, N. Harashima, M. Tongu, Y. Tamaki, N. Uchida, T. Inomata and M. Harada, Pifithrin-μ, an inhibitor of heat-shock protein 70, can increase the antitumor effects of hyperthermia against human prostate cancer cells, *PLoS One*, 2013, **8**, e78772, DOI: 10.1371/journal.pone.0078772.

86 S. Khoei, M. Azarian and M. Rafipour, The effect of quercetin and hyperthermia on spheroid model of du145 prostate carcinoma cell line, *J. Paramed. Sci.*, 2013, **4**, 82–89, DOI: 10.22037/jps.v4i2.4490.

87 H. Machida, S. Nakajima, N. Shikano, J. Nishio, S. Okada, M. Asayama, M. Shirai and N. Kubota, Heat shock protein 90 inhibitor 17-allylamino-17-demethoxygeldanamycin potentiates the radiation response of tumor cells grown as monolayer cultures and spheroids by inducing apoptosis, *Cancer Sci.*, 2005, **96**, 911–917, DOI: 10.1111/j.1349-7006.2005.00125.x.

88 R. Yang, Q. Tang, F. Miao, Y. An, M. Li, Y. Han, X. Wang, J. Wang, P. Liu and R. Chen, Inhibition of heat-shock protein 90 sensitizes liver cancer stem-like cells to magnetic hyperthermia and enhances anti-tumor effect on hepatocellular carcinoma-burdened nude mice, *Int. J. Nanomed.*, 2015, **10**, 7345–7358, DOI: 10.2147/IJN.S93758.

89 L. E. M. Vriend, N. van den Tempel, A. L. Oei, M. L'Acosta, F. J. Pieterson, N. A. P. Franken, R. Kanaar and P. M. Krawczyk, Boosting the effects of hyperthermia-based anticancer treatments by HSP90 inhibition, *Oncotarget*, 2017, **8**, 97490–97503, DOI: 10.18632/oncotarget.22142.

90 S. Stangl, M. Gehrmann, J. Riegger, K. Kuhs, I. Riederer, W. Sievert, K. Hube, R. Mocikat, R. Dressel, E. Kremmer, A. G. Pockley, L. Friedrich, L. Vigh, A. Skerra and G. Multhoff, Targeting membrane heat-shock protein 70 (Hsp70) on tumors by cmHsp70.1 antibody, *Proc. Natl. Acad. Sci. U. S. A.*, 2011, **108**, 733–738, DOI: 10.1073/pnas.1016065108.

91 E. A. Taha, K. Ono and T. Eguchi, Roles of extracellular HSPs as biomarkers in immune surveillance and immune evasion, *Int. J. Mol. Sci.*, 2019, **20**, 4588, DOI: 10.3390/ijms20184588.

92 M. Matokanovic, K. Barisic, J. Filipovic-Grcic and D. Maysinger, Hsp70 silencing with siRNA in nanocarriers enhances cancer cell death induced by the inhibitor of Hsp90, *Eur. J. Pharm. Sci.*, 2013, **50**, 149–158, DOI: 10.1016/j.ejps.2013.04.001.

93 N. A. Stocke, P. Sethi, A. Jyoti, R. Chan, S. M. Arnold, J. Z. Hilt and M. Upreti, Toxicity evaluation of magnetic hyperthermia induced by remote actuation of magnetic nanoparticles in 3D micrometastasic tumor tissue analogs for triple negative breast cancer, *Biomaterials*, 2017, **120**, 115–125, DOI: 10.1016/j.biomaterials.2016.12.019.

94 S. Ullah, K. Seidel, S. Türkkan, D. P. Warwas, T. Dubich, M. Rohde, H. Hauser, P. Behrens, A. Kirschning, M. Köster and D. Wirth, Macrophage entrapped silica coated superparamagnetic iron oxide particles for controlled drug release in a 3D cancer model, *J. Controlled Release*, 2019, **294**, 327–336, DOI: 10.1016/j.jconrel.2018.12.040.

95 X. Peng, B. Wang, Y. Yang, Y. Zhang, Y. Liu, Y. He, C. Zhang and H. Fan, Liver tumor spheroid reconstitution for testing mitochondrial targeted magnetic hyperthermia treatment, *ACS Biomater. Sci. Eng.*, 2019, **5**, 1635–1644, DOI: 10.1021/acsbiomaterials.8b01630.

96 S. Piehler, L. Wucherpfennig, F. L. Tansi, A. Berndt, R. Quaas, U. Teichgraeber and I. Hilger, Hyperthermia affects collagen fiber architecture and induces apoptosis in pancreatic and fibroblast tumor hetero-spheroids *in vitro*, *Nanomedicine*, 2020, **28**, 102183, DOI: 10.1016/j.nano.2020.102183.

97 C. Ricci, L. Moroni and S. Danti, Cancer tissue engineering—new perspectives in understanding the biology of solid tumours—a critical review, *OA Tissue Eng*, 2013, **1**, 4.

98 W. M. Pardridge, Biopharmaceutical drug targeting to the brain, *J. Drug Targeting*, 2010, **18**, 157–167, DOI: 10.3109/10611860903548354.

99 J. J. Jamieson, P. C. Searson and S. Gerecht, Engineering the human blood-brain barrier *in vitro*, *J. Biol. Eng.*, 2017, **11**, 37, DOI: 10.1186/s13036-017-0076-1.

100 D. F. Emerich, R. L. Dean, C. Osborn and R. T. Bartus, The development of the bradykinin agonist labradimil as a means to increase the permeability of the blood-brain barrier: from concept to clinical evaluation, *Clin. Pharmacokinet.*, 2001, **40**, 105–123, DOI: 10.2165/00003088-200140020-00003.

101 S. Dohgu, F. Takata, A. Yamauchi, S. Nakagawa, T. Egawa, M. Naito, T. Tsuruo, Y. Sawada, M. Niwa and Y. Kataoka, Brain pericytes contribute to the induction and up-regulation of blood-brain barrier functions through transforming growth factor-beta production, *Brain Res.*, 2005, **1038**, 208–215, DOI: 10.1016/j.brainres.2005.01.027.

102 R. Cecchelli, V. Berezowski, S. Lundquist, M. Culot, M. Renftel, M. P. Dehouck and L. Fenart, Modelling of the blood-brain barrier in drug discovery and development, *Nat. Rev. Drug Discovery*, 2007, **6**, 650–661, DOI: 10.1038/nrd2368.

103 O. O. Ogunshola, *In vitro* modeling of the blood-brain barrier: simplicity *versus* complexity, *Curr. Pharm. Des.*, 2011, **17**, 2755–2761, DOI: 10.2174/138161211797440159.

104 M. Urakawa, K. Yamaguchi, E. Tsuchida, S. Kashiwagi, H. Ito and T. Matsuda, Blood-brain barrier disturbance following localized hyperthermia in rats, *Int. J. Hyperthermia*, 1995, **11**, 709–718, DOI: 10.3109/02656739509022502.

105 A. J. Giustini, A. A. Petryk, S. M. Cassim, J. A. Tate, I. Baker and P. J. Hoopes, Magnetic nanoparticle hyperthermia in cancer treatment, *Nano LIFE*, 2010, **1**, 17–32, DOI: 10.1142/S1793984410000067.

106 M. Dan, Y. Bae, T. A. Pittman and R. A. Yokel, Alternating magnetic field-induced hyperthermia increases iron oxide nanoparticle cell association/uptake and flux in blood-brain barrier models, *Pharm. Res.*, 2015, **32**, 1615–1625, DOI: 10.1007/s11095-014-1561-6.

107 S. N. Tabatabaei, M. S. Tabatabaei, H. Girouard and S. Martel, Hyperthermia of magnetic nanoparticles allows passage of sodium fluorescein and Evans blue dye across the blood-retinal barrier, *Int. J. Hyperthermia*, 2016, **32**, 657–665, DOI: 10.1080/02656736.2016.1193903.

108 A. Pandey, K. Singh, S. Patel, R. Singh, K. Patel and K. Sawant, Hyaluronic acid tethered pH-responsive alloy-drug nanoconjugates for multimodal therapy of glioblastoma: An intranasal route approach, *Mater. Sci. Eng., C*, 2019, **98**, 419–436, DOI: 10.1016/j.msec.2018.12.139.

109 C. L. Chaffer and R. A. Weinberg, A perspective on cancer cell metastasis, *Science*, 2011, **331**, 1559–1564, DOI: 10.1126/science.1203543.

110 C. Walker, E. Mojares and A. Del Río Hernández, Role of extracellular matrix in development and cancer progression, *Int. J. Mol. Sci.*, 2018, **19**, 3028, DOI: 10.3390/ijms19103028.

111 T. Kumeria, S. Maher, Y. Wang, G. Kaur, L. Wang, M. Erkelens, P. Forward, M. F. Lambert, A. Evdokiou and D. Losic, Naturally derived iron oxide nanowires from bacteria for magnetically triggered drug release and cancer hyperthermia in 2D and 3D culture environments: bacteria biofilm to potent cancer therapeutic, *Biomacromolecules*, 2016, **17**, 2726–2736, DOI: 10.1021/acs.biomac.6b00786.

112 L. Beola, L. Asín, R. M. Fratila, V. Herrero, J. M. de la Fuente, V. Grazú and L. Gutiérrez, Dual role of magnetic nanoparticles as intracellular hotspots and extracellular matrix disruptors triggered by magnetic hyperthermia in 3D cell culture models, *ACS Appl. Mater. Interfaces*, 2018, **10**, 44301–44313, DOI: 10.1021/acsami.8b18270.

113 Y. Zhang, D. Zhai, M. Xu, Q. Yao, J. Chang and C. Wu, 3D-printed bioceramic scaffolds with a Fe_3O_4/graphene oxide nanocomposite interface for hyperthermia therapy of bone tumor cells, *J. Mater. Chem. B*, 2016, **4**, 2874–2886, DOI: 10.1039/C6TB00390G.

114 K. N. Han, C. A. Li and G. H. Seong, Microfluidic chips for immunoassays, *Annu. Rev. Anal. Chem.*, 2013, **6**, 119–141, DOI: 10.1146/annurev-anchem-062012-092616.

115 K. Shaw, Y. H. Nai and S. Haswell, Application of microfluidic methodology for the analysis of DNA, *Micromachines*, 2018, **9**, 18, DOI: 10.3390/mi9010018.

116 C. Regnault, D. S. Dheeman and A. Hochstetter, Microfluidic devices for drug assays, *High-Throughput*, 2018, **7**, 18, DOI: 10.3390/ht7020018.

117 J. E. Sosa-Hernández, A. M. Villalba-Rodríguez, K. D. Romero-Castillo, M. A. Aguilar-Aguila-Isaías, I. E. García-Reyes, A. Hernández-Antonio, I. Ahmed, A. Sharma, R. Parra-Saldívar and H. M. N. Iqbal, Organs-on-a-Chip module: A review from the development and

applications perspective, *Micromachines*, 2018, **9**, 536, DOI: 10.3390/mi9100536.

118 G. Luka, A. Ahmadi, H. Najjaran, E. Alocilja, M. DeRosa, K. Wolthers, A. Malki, H. Aziz, A. Althani and M. Hoorfar, Microfluidics integrated biosensors: a leading technology towards lab-on-a-chip and sensing applications, *Sensors*, 2015, **15**, 30011–30031, DOI: 10.3390/s151229783.

119 V. S. Shirure, Y. Bi, M. B. Curtis, A. Lezia, M. W. Goedegebuure, S. P. Goedegebuure, R. Aft, R. C. Fields and S. C. George, Tumor-on-a-chip platform to investigate progression and drug sensitivity in cell lines and patient-derived organoids, *Lab Chip*, 2018, **18**, 3687–3702, DOI: 10.1039/c8lc00596f.

120 D. Kalinowska, I. Grabowska-Jadach, M. Liwinska, M. Drozd, M. Pietrzak, A. Dybko and Z. Brzozka, Studies on effectiveness of PTT on 3D tumor model under microfluidic conditions using aptamer-modified nanoshells, *Biosens. Bioelectron.*, 2019, **126**, 214–221, DOI: 10.1016/j.bios.2018.10.069.

121 M. Weinhart, A. Hocke, S. Hippenstiel, J. Kurreck and S. Hedtrich, 3D organ models-Revolution in pharmacological research?, *Pharmacol. Res.*, 2019, **139**, 446–451, DOI: 10.1016/j.phrs.2018.11.002.

122 J. B. Mamani, B. S. Marinho, G. N. A. Rego, M. P. Nucci, F. Alvieri, R. S. dos Santos, J. V. M. Ferreira, F. A. de Oliveira and L. F. Gamarra, Magnetic hyperthermia therapy in glioblastoma tumor on-a-Chip model, *Einstein*, 2020, **18**, eAO4954, DOI: 10.31744/einstein_journal/2020AO4954.